Politecnico di Torino

Department of Electronics and Telecommunications

Attitude control system for nanosatellites with reaction wheel and magnetorquer actuators

By:

Sevil Mohammadzadeh Sadigh

Supervisor:

Prof. Leonardo Reyneri

List of parameters

$\mathbf{I}_S$	The matrix of the inertia tensor of satellite
I_w	Inertia momentum of Reaction wheels
X_I, Y_I, Z_I	Earth Center Inertial coordinate frame (ECI)
X_O, Y_O, Z_O	Orbital coordinate frame
X_B, Y_B, Z_B	Body-Fixed coordinate frame
E	Eccentricity
A	Semi-major axis
R_A	apogee/ periapsis
R_P	perigee/ apoapsis
i	Inclination
☊ or Ω	Longitude of the ascending node
Ω	Argument of periapsis
v	True anomaly
ω_0	the orbital rotation frequency
G	the gravitational constant
M_e	the Mass of the earth
R	the distance from the center of the earth
R_E	the Earth radius
H	the distance of the satellite from the earth
m	the magnetic dipole strength
φ	the rotation about the x body axis — Euler angles
θ	the rotation about the y body axis — Euler angles
ψ	the rotation about the z body axis — Euler angles
$\bar{\mathbf{q}}$	Quaternion
q_0	scalar part of the quaternion
$\mathbf{q}=(q_1, q_2, q_3)$	vector part of the quaternion
$\mathbf{C}$	Rotation matrix
$\mathbf{T}$	External torques applied to the satellite
H	total angular momentum of the satellite
ω_{bi}	the angular velocity of the body-fixed reference with respect to the inertial frame
$\mathbf{T_c}$	Control torque generated by the controller

$\mathbf{T_d}$	External disturbance torque
h_w	angular momentum of the wheel
D	wheel orientation matrix
T_w	Control torque generated by reaction wheel
$\bar{\mathbf{q}}_d$	desired quaternion

This work has been done by Sevil M. Sadigh under supervision of Professor Leonardo Reyneri at the Polytechnic University of Turin[1], Italy. Sevil M. Sadigh is PhD student from Iran and she is doing her PhD thesis, at the moment. A part of her thesis is about satellite attitude control. She has worked on this part of her PhD thesis at the Department of Electronics and Telecommunications, as a visiting research scholar for a period of six months, from May 5th to Nov 5th 2017.

The works done in this period is described in this text as follows. In section 1, coordinate frames such as inertia, body, and orbit are described to determine the satellite attitude. Some types of orbital classifications like as centric classifications, altitude classifications for geocentric orbits, eccentricity classifications, and inclination classifications are described in section 2. Also, some necessary information like as orbital elements, orbital period and earth magnetic field are explained. In section 3, satellite attitude and the types of the rotation are described. Also, how to convert them to each other are explained. Then satellite kinematic and dynamic equations are described in section 4. Attitude actuators, their characteristics, advantages and disadvantages and their operations are explained in section 5. Attitude control is described in section 6. Attitude control approach used in this work is SMC[2]. SMC method is explained its advantages and disadvantages is described then the controller is designed for satellite attitude control with magnetorquer and reaction wheel actuators, in this section. In section 7, the proposed attitude control is simulated for the nanosatellites with several combinations of the actuators. At first, a sample attribute motion for tracking has been described. Then, attitude dynamic and kinematic of the satellite has been explained. The numerical model for the attitude control has been described in the next section. Finally, the performed simulations are explained. In the final section, the conclusion and future works are described.

[1] Politecnico di Torino

[2] Sliding Mode Control

Contents

1. Common reference frames 1

1-1. Earth-Centered Inertial Frame (ECI) 1

1-2. Sat-Centered Inertial Frame (SCI) 1

1-3. Orbital Frame 2

1-4. Body-Fixed Frame 2

2. Satellite orbits 3

2-1. Centric classifications 3

2-2. Orbital elements 3

2-3. Eccentricity classifications 5

2-4. Altitude classifications for geocentric orbits 5

2-5. Inclination classifications 6

2-6. Orbital period 6

2-7. Magnetic field of earth 6

3. Satellite Attitude 7

3-1. Euler angles 7

3-2. Axis + angle 7

3-3. Rotation matrix 8

3-4. Quaternion 9

3-5. Euler Angles to Quaternion conversion 9

3-6. Quaternion to Euler angles conversion 10

4. Satellite Kinematics and Dynamics 10

4-1. Attitude dynamics 10

4-2. Attitude kinematics 11

5. Attitude Actuators.. 12

5-1. Magnetorquer 12

5-2. Reaction Wheel 14

6. Attitude Control 15

6-1. Sliding Mode Control.. 15

6-2. SMC design for satellite attitude control... 18

6-2-1. Satellite attitude control with magnetorquer actuator 19

6-2-2. Satellite attitude control with reaction wheel actuator.................................. 20

7. Simulation examples.. 21

7-1. Desired Motion.. 21

7-2. The numerical model of the satellite 21

7-3. Describing simulation satellite attitude models 22

7-4. Describing actuator model 23

7-5. Simulations.. 25

7.5.1. Simulation results by one magnetorquer 26

7.5.2. Simulation results by two magnetorquers.. 29

7.5.3. Simulation results by one Reaction Wheel 33

7.5.4. Simulation results by three reaction wheels 36

7.5.5. Simulation results by one reaction wheel and three magnetorquers............... 39

8. Conclusion and future works... 43

List of Figures

FIGURE 1-1: EARTH-CENTERED INERTIAL FRAME [2] 1
FIGURE 1-2: SAT-CENTERED INERTIAL FRAME (SCI) [2] 1
FIGURE 1-3: ORBITAL FRAME [2] 2
FIGURE 1-4: BODY-FIXED FRAME [2] 2
FIGURE 2-1: ECCENTRICITY AND SEMI-MAJOR AXIS [2] 4
FIGURE 2-2: KEPLERIAN ELEMENTS [5] 5
FIGURE 3-1: AXIS + ANGLE OR EULER AXIS 8
FIGURE 3-2: THE ORIENTATION OF THE THREE AXES U, V, W IN THE REFERENCE FRAME X, Y, Z 8
FIGURE 5-1: A SAMPLE OF MAGNETORQUER [13] 13
FIGURE 5-2: A SAMPLE OF REACTION WHEEL [17] 14
FIGURE 6-1: GRAPHICAL INTERPRETATION OF EQUATIONS (2) AND (5), (N=2) [18] 17
FIGURE 6-2: CHATTERING AS A RESULT OF IMPERFECT CONTROL SWITCHING MODIFIED [18] 18
FIGURE 7-1: ATTITUDE DYNAMIC AND KINEMATIC MODELS 22
FIGURE 7-2: SATELLITE ATTITUDE DYNAMIC 22
FIGURE 7-3: SATELLITE ATTITUDE KINEMATIC 23
FIGURE 7-4: MAGNETORQUER MODEL 23
FIGURE 7-5: REACTION WHEEL MODEL 24
FIGURE 7-6: MODIFIED ATTITUDE DYNAMIC SATELLITE WITH REACTION WHEELS 25
FIGURE 7-7: (A) DESIRED ANGLE AND ROTATION ANGLE ABOUT Y-AXIS (Θ), (B) ANGULAR VELOCITY, (C) INPUT CONTROL TORQUE AND TORQUE GENERATED IN THE SATELLITE 26
FIGURE 7-8: DESIRED ANGLE AND ROTATION ANGLE ABOUT X-AXIS (Φ), (B) ANGULAR VELOCITY, (C) INPUT CONTROL TORQUE AND TORQUE GENERATED IN THE SATELLITE 27
FIGURE 7-9: (A) DESIRED ANGLE AND ROTATION ANGLE ABOUT Z-AXIS (Ψ), (B) ANGULAR VELOCITY, (C) INPUT CONTROL TORQUE AND TORQUE GENERATED IN THE SATELLITE 27
FIGURE 7-10: THE MAGNETORQUER CURRENTS LAID ON THE (A) X-AXIS, (B) Y-AXIS AND (C) Z-AXIS 27
FIGURE 7-11: (A) DESIRED ANGLE AND ROTATION ANGLE ABOUT Y-AXIS (Θ), (B) ANGULAR VELOCITY, (C) INPUT CONTROL TORQUE AND TORQUE GENERATED IN THE SATELLITE 28
FIGURE 7-12: (A) DESIRED ANGLE AND ROTATION ANGLE ABOUT X-AXIS (Φ), (B) ANGULAR VELOCITY, (C) INPUT CONTROL TORQUE AND TORQUE GENERATED IN THE SATELLITE 28
FIGURE 7-13: (A) DESIRED ANGLE AND ROTATION ANGLE ABOUT Z-AXIS (Ψ), (B) ANGULAR VELOCITY, (C) INPUT CONTROL TORQUE AND TORQUE GENERATED IN THE SATELLITE 29
FIGURE 7-14: THE MAGNETORQUER CURRENTS LAID ON THE (A) X-AXIS, (B) Y-AXIS, (C) Z-AXIS 29
FIGURE 7-15: (A) DESIRED ANGLE AND ROTATION ANGLE ABOUT Y-AXIS (Θ), (B) ANGULAR VELOCITY, (C) INPUT CONTROL TORQUE AND TORQUE GENERATED IN THE SATELLITE 30
FIGURE 7-16: (A) DESIRED ANGLE AND ROTATION ANGLE ABOUT X-AXIS (Φ), (B) ANGULAR VELOCITY, (C) INPUT CONTROL TORQUE AND TORQUE GENERATED IN THE SATELLITE 30
FIGURE 7-17: (A) DESIRED ANGLE AND ROTATION ANGLE ABOUT Z-AXIS (Ψ), (B) ANGULAR VELOCITY, (C) INPUT CONTROL TORQUE AND TORQUE GENERATED IN THE SATELLITE 30

FIGURE 7-18: THE MAGNETORQUER CURRENTS LAID ON THE (A) X-AXIS, (B) Y-AXIS, (C) Z-AXIS 31
FIGURE 7-19: (A) DESIRED ANGLE AND ROTATION ANGLE ABOUT Y-AXIS (Θ), (B) ANGULAR VELOCITY, (C) INPUT CONTROL TORQUE AND TORQUE GENERATED IN THE SATELLITE..31
FIGURE 7-20: (A) DESIRED ANGLE AND ROTATION ANGLE ABOUT X-AXIS (Φ), (B) ANGULAR VELOCITY, (C) INPUT CONTROL TORQUE AND TORQUE GENERATED IN THE SATELLITE..32
FIGURE 7-21: (A) DESIRED ANGLE AND ROTATION ANGLE ABOUT Z-AXIS (Ψ), (B) ANGULAR VELOCITY, (C) INPUT CONTROL TORQUE AND TORQUE GENERATED IN THE SATELLITE..32
FIGURE 7-22: THE MAGNETORQUER CURRENTS LAID ON THE (A) X-AXIS, (B) Y-AXIS, (C) Z-AXIS 32
FIGURE 7-23: DESIRED ANGLE 33
FIGURE 7-24: SLIDER GAIN 33
FIGURE 7-25: (A) DESIRED ANGLE AND ROTATION ANGLE ABOUT Y-AXIS (Θ), (B) ANGULAR VELOCITY, (C) INPUT CONTROL TORQUE AND REACTION WHEEL TORQUE, (D) REACTION WHEEL MOMENTUM......................................34
FIGURE 7-26: (A) DESIRED ANGLE AND ROTATION ANGLE ABOUT X-AXIS (Φ), (B) ANGULAR VELOCITY, (C) INPUT CONTROL TORQUE AND REACTION WHEEL TORQUE, (D) REACTION WHEEL MOMENTUM......................................34
FIGURE 7-27: (A) DESIRED ANGLE AND ROTATION ANGLE ABOUT Z-AXIS (Ψ), (B) ANGULAR VELOCITY, (C) INPUT CONTROL TORQUE AND REACTION WHEEL TORQUE, (D) REACTION WHEEL MOMENTUM......................................35
FIGURE 7-28: (A) DESIRED ANGLE AND ROTATION ANGLE ABOUT Y-AXIS (Θ), (B) ANGULAR VELOCITY, (C) INPUT CONTROL TORQUE AND REACTION WHEEL TORQUE, (D) REACTION WHEEL MOMENTUM......................................35
FIGURE 7-29: (A) DESIRED ANGLE AND ROTATION ANGLE ABOUT Z-AXIS (Ψ), (B) ANGULAR VELOCITY, (C) INPUT CONTROL TORQUE AND REACTION WHEEL TORQUE, (D) REACTION WHEEL MOMENTUM......................................36
FIGURE 7-30: (A) DESIRED ANGLE AND ROTATION ANGLE ABOUT Y-AXIS (Θ), (B) ANGULAR VELOCITY, (C) INPUT CONTROL TORQUE AND REACTION WHEEL TORQUE, (D) REACTION WHEEL MOMENTUM......................................37
FIGURE 7-31: (A) DESIRED ANGLE AND ROTATION ANGLE ABOUT X-AXIS (Φ), (B) ANGULAR VELOCITY, (C) INPUT CONTROL TORQUE AND REACTION WHEEL TORQUE, (D) REACTION WHEEL MOMENTUM......................................37
FIGURE 7-32: (A) DESIRED ANGLE AND ROTATION ANGLE ABOUT Z-AXIS (Ψ), (B) ANGULAR VELOCITY, (C) INPUT CONTROL TORQUE AND REACTION WHEEL TORQUE, (D) REACTION WHEEL MOMENTUM......................................38
FIGURE 7-33: (A) DESIRED ANGLE AND ROTATION ANGLE ABOUT Y-AXIS (Θ), (B) ANGULAR VELOCITY, (C) INPUT CONTROL TORQUE AND REACTION WHEEL TORQUE, (D) REACTION WHEEL MOMENTUM......................................38
FIGURE 7-34: (A) DESIRED ANGLE AND ROTATION ANGLE ABOUT X-AXIS (Φ), (B) ANGULAR VELOCITY, (C) INPUT CONTROL TORQUE AND REACTION WHEEL TORQUE, (D) REACTION WHEEL MOMENTUM......................................39
FIGURE 7-35: (A) DESIRED ANGLE AND ROTATION ANGLE ABOUT Y-AXIS (Θ), (B) ANGULAR VELOCITY, (C) INPUT CONTROL TORQUE AND TORQUE GENERATED IN THE SATELLITE..40
FIGURE 7-36: (A) DESIRED ANGLE AND ROTATION ANGLE ABOUT X-AXIS (Φ), (B) ANGULAR VELOCITY, (C) INPUT CONTROL TORQUE AND TORQUE GENERATED IN THE SATELLITE..40
FIGURE 7-37: (A) DESIRED ANGLE AND ROTATION ANGLE ABOUT Z-AXIS (Ψ), (B) ANGULAR VELOCITY, (C) INPUT CONTROL TORQUE AND TORQUE GENERATED IN THE SATELLITE..41
FIGURE 7-38: THE MAGNETORQUER CURRENTS LAID ON THE (A) X-AXIS, (B) Y-AXIS, (C) Z-AXIS 41
FIGURE 7-39: (A) DESIRED ANGLE AND ROTATION ANGLE ABOUT Y-AXIS (Θ), (B) ANGULAR VELOCITY, (C) INPUT CONTROL TORQUE AND MAGNETORQUER TORQUE, (D) REACTION WHEEL TORQUE, (E) REACTION WHEEL MOMENTUM...42
FIGURE 7-40: (A) DESIRED ANGLE AND ROTATION ANGLE ABOUT X-AXIS (Φ), (B) ANGULAR VELOCITY, (C) INPUT CONTROL TORQUE AND MAGNETORQUER TORQUE..42

FIGURE 7-41: (A) DESIRED ANGLE AND ROTATION ANGLE ABOUT Z-AXIS (Ψ), (B) ANGULAR VELOCITY, (C) INPUT CONTROL TORQUE AND MAGNETORQUER TORQUE 43
FIGURE 7-42: THE MAGNETORQUER CURRENTS LAID ON THE (A) X-AXIS, (B) Y-AXIS, (C) Z-AXIS 43

1. Common reference frames

In this section, conventional coordinate frames such as inertia, body, and orbit are described to determine the satellite attitude.

1-1. Earth-Centered Inertial Frame (ECI)

ECI coordinate frames have their origins at the center of mass of the Earth. The ECI coordinate system does not rotate with the rotation of the earth. The x-y plane coincides with the Earth's equatorial plane. X-axis is permanently fixed and corresponds to the vernal equinox. Z-axis lies at a 90 angle to the equatorial plane and extends through the North Pole. Y-axis is also obtained using the right hand rule. It is used to determine satellite attitude [1].

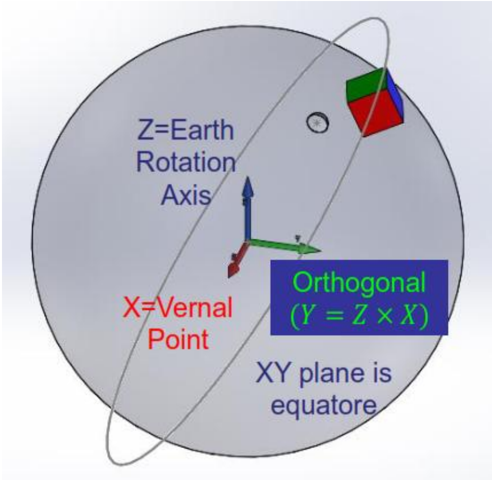

Figure 1-1: Earth-Centered Inertial Frame [2]

1-2. Sat-Centered Inertial Frame (SCI)

The origin of SCI coordinate frame is located on the orbit. Its axes are parallel with the axes of ECI. It moves with the satellite.

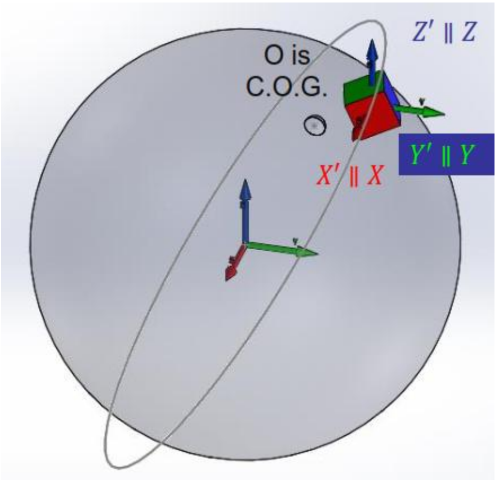

Figure 1-2: Sat-Centered Inertial Frame (SCI) [2]

Where C.O.G. is a point of a satellite exactly remains on the orbit and exactly follows the rules of gravity.

1-3. Orbital Frame

The origin of the orbital coordinate frame is located at the center of the mass of the satellite. Z-axis is toward the center of the earth. Y-axis is orthogonal to the satellite's orbit. X-axis is obtained by using the right hand rule.

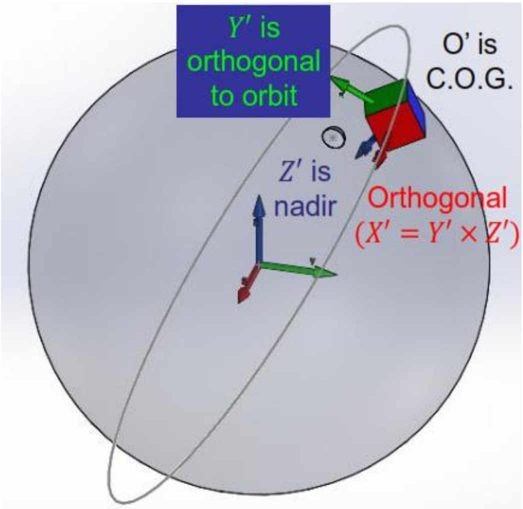

Figure 1-3: orbital frame [2]

1-4. Body-Fixed Frame

The origin of the body's coordinates is located at the center of the satellite and rotated through it. This frame sticks to the body of the satellite. The axes are chosen arbitrarily, but usually Z-axis is heading direction for telescope, Y-axis is antenna principal direction and it is orthogonal to Z-axis and X-axis is obtained by using the right hand rule.

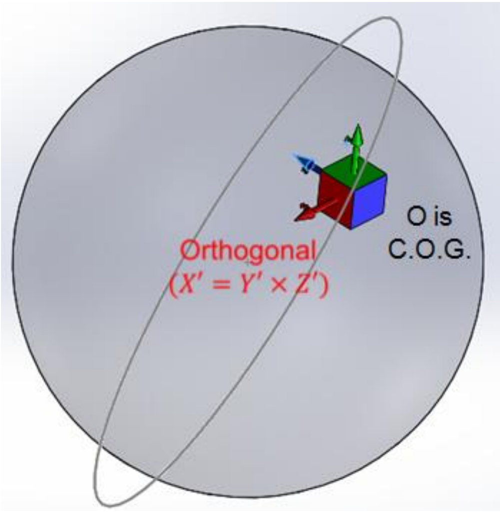

Figure 1-4: Body-Fixed Frame [2]

2. Satellite orbits

There are several types of orbital classifications like as centric classifications, altitude classifications for geocentric orbits, eccentricity classifications, inclination classifications and etc. in this section, some classifications are described. It is obvious that it may never be able to satisfy particular standards for completeness.

2-1. Centric classifications

This classification is based on orbit center [3].

- Heliocentric orbit: An orbit around the Sun. In the Solar System, all planets, comets, and asteroids are in such orbits, as are many artificial satellites and pieces of space debris. Moons by contrast are not in a heliocentric orbit but rather orbit their parent object.
- Geocentric orbit: An orbit around the planet Earth, such as that of the Moon or of artificial satellites.
- Areocentric orbit: An orbit around the planet Mars, such as that of its moons or artificial satellites.
- Lunar orbit: An orbit around the Earth's moon.
- Hermocentric orbit: An orbit around the planet Mercury.
- Aphrodiocentric orbit: An orbit around the planet Venus.
- Jovicentric orbit: An orbit around the planet Jupiter.
- Kronocentric orbit: An orbit around the planet Saturn.
- Oranocentric orbit: An orbit around the planet **Uranus**.

2-2. Orbital elements

Orbital elements are the parameters that define location of orbits in space [4]. There are many different ways to mathematically describe the same orbit, but certain schemes, each consisting of a set of six parameters, are commonly used in astronomy and orbital mechanics [5].

A real orbit (and its elements) changes over time due to gravitational perturbations by other objects and the effects of relativity. A Keplerian orbit is merely an idealized, mathematical approximation at a particular time. There are six parameters to define the location in space of a body moving in any Keplerian orbit. These parameters are known as the classical orbit parameters.

The main two elements that define the shape and size of the ellipse:

- **Eccentricity (*e*)**: shape of the ellipse, describing how much it is elongated compared to a circle. It is defined as

$$e = \frac{R_A - R_P}{R_A + R_P} \tag{2-1}$$

Where R_A is apogee/ periapsis and R_P is perigee/ apoapsis.

- **Semi-major axis (*a*)**: the sum of the periapsis and apoapsis distances divided by two. For circular orbits, the semimajor axis is the distance between the centers of the bodies, not the distance of the bodies from the center of mass. For paraboles or hyperboles, this is infinite. It is defined as

$$a = \frac{R_A + R_P}{2} \tag{2-2}$$

These parameters are shown in Figure 2-1.

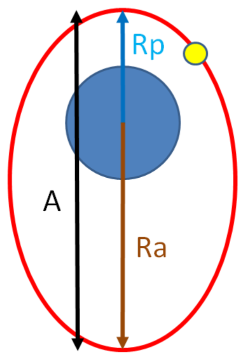

Figure 2-1: Eccentricity and semi-major axis [2]

Two elements define the orientation of the orbital plane in which the ellipse is embedded:

- **Inclination (i)**: vertical tilt of the ellipse with respect to the reference plane, measured at the ascending node (where the orbit passes upward through the reference plane, the green angle *i* in Figure 2-2).

- **Longitude of the ascending node (☊ or *Ω*)**: horizontally orients the ascending node of the ellipse (where the orbit passes upward through the reference plane) with respect to the reference frame's vernal point (the green angle *Ω* in Figure 2-2).

And finally:

- **Argument of periapsis (*ω*)**: defines the orientation of the ellipse in the orbital plane, as an angle measured from the ascending node to the periapsis (the closest point the satellite object comes to the primary object around which it orbits, the blue angle *ω* in Figure 2-2).

- **True anomaly (*ν*, *θ*, or *f*) at epoch (M_0)**: defines the position of the orbiting body along the ellipse at a specific time (the "epoch").

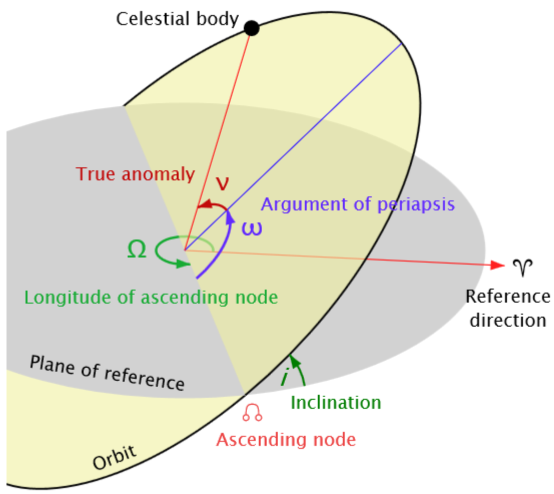

Figure 2-2: Keplerian elements [5]

2-3. Eccentricity classifications

There are two types of orbits: closed (periodic) orbits, and open (escape) orbits. Circular and elliptical orbits are closed. Parabolic and hyperbolic orbits are open. Radial orbits can be either open or closed. This classification is based on eccentricity [6, 7]:

- **Circular orbit**: An orbit that has an eccentricity of 0 and whose path traces a circle.
- **Elliptic orbit**: An orbit with an eccentricity greater than 0 and less than 1 whose orbit traces the path of an ellipse.
- **Parabolic orbit**: An orbit with the eccentricity equal to 1. Such an orbit also has a velocity equal to the escape velocity and therefore will escape the gravitational pull of the planet. If the speed of a parabolic orbit is increased it will become a hyperbolic orbit.
- **Hyperbolic orbit**: An orbit with the eccentricity greater than 1. Such an orbit also has a velocity in excess of the escape velocity and as such, will escape the gravitational pull of the planet and continue to travel infinitely until it is acted upon by another body with sufficient gravitational force.
- **Radial orbit**: An orbit with zero angular momentum and eccentricity equal to 1. The two objects move directly towards or away from each other in a straight-line.
- **Decaying orbit**: A decaying orbit is one with a minimum distance between the two objects that decreases over time due to factors like atmospheric resistance. Often used to dispose of dying artificial satellites.

2-4. Altitude classifications for geocentric orbits

This classification is based on orbit altitude from the earth [6, 7].

- **Low Earth orbit (LEO)**: geocentric orbits with altitudes from 160 to 2,000 km.

- **Medium Earth orbit (MEO)**: geocentric orbits ranging in altitude from 2,000 km to just below geosynchronous orbit at 35,786 kilometers.
- Both geosynchronous orbit (GSO) and geostationary orbit (GEO) are orbits around Earth matching Earth's sidereal rotation period. All geosynchronous and geostationary orbits have a semi-major axis of 42,164 km. This works out to an altitude of 35,786 km. All geostationary orbits are also geosynchronous, but not all geosynchronous orbits are geostationary. A geostationary orbit stays exactly above the equator, whereas a geosynchronous orbit may swing north and south to cover more of the Earth's surface. Both complete one full orbit of Earth per sidereal day (relative to the stars, not the Sun).
- **High Earth orbit**: geocentric orbits above the altitude of geosynchronous orbit 35,786 km

2-5. Inclination classifications

This classification is based on inclination orbit angle [7, 8].

- **Inclined orbit**: An orbit whose inclination in reference to the equatorial plane is not zero.
- **Non-inclined orbit**: An orbit whose inclination is equal to zero with respect to some plane of reference.

2-6. Orbital period

In this work, the orbital period is the time a satellite takes to complete one orbit around the earth. The orbital rotation frequency (ω_0) is

$$\omega_0 = \sqrt{\frac{G.M_e}{\mathrm{R}^3}} \qquad \textbf{(2-3)}$$

Where G is gravitational constant, M_e is the Mass of earth and R is the distance from center of the earth (R_E + h). R_E is the Earth radius and h is the distance of the satellite from the earth [9].

2-7. Magnetic field of earth

The Earth's magnetic field is predominantly that of a magnetic dipole such as that produced by a sphere of uniform magnetization or a current loop [9]. Its intensity is proportional to m/R^3, where *R* is the distance from the center of the earth and *m* is the magnetic dipole strength. Thus, the strength of the magnetic field decreases strongly with the altitude of the satellite [4].

A simplified model of the earth's magnetic field, with respect to the orbital coordinate frame is given as (see Figure 2-2)

$$\begin{bmatrix} B_{xo} \\ B_{yo} \\ B_{zo} \end{bmatrix} = \frac{m}{R^3} \begin{bmatrix} \cos(\alpha - \omega_0 t)\sin(i) \\ \cos(i) \\ -2\cos(\alpha - \omega_0 t)\sin(i) \end{bmatrix} \tag{2-4}$$

Where α = (ω + υ), R is the distance from the center of the earth and *m* is the magnetic dipole strength.

3. Satellite Attitude

Satellite attitude is defined as the rotation from satellite centered inertial frame to Body-Fixed frame. The rotations are defined mathematically as

1. Euler angles
2. Axis + angle
3. Rotation matrix
4. Quaternion

3-1. Euler angles

The Euler angle rotation is defined as successive angular rotations about the three orthogonal frame axes [4]. Any orientation can be achieved by composing three elemental rotations, i.e. rotations about the axes of a coordinate system. Euler angles can be defined by three of these rotations [2].

It is common to define the Euler roll angle (φ) as a rotation about the x body axis, the pitch angle *(θ)* about the y body axis, and the yaw angle *(ψ)* about the z body axis.

There are twelve possible sequences of rotation axes, divided in two groups:

- Proper Euler angles (*z-x-z, x-y-x, y-z-y, z-y-z, x-z-x, y-x-y*)
- Tait–Bryan angles (*x-y-z, y-z-x, z-x-y, x-z-y,* ***z-y-x****, y-x-z*)

Tait–Bryan angles are also called **yaw, pitch, and roll**. Sometimes, both kinds of sequences are called "Euler angles". In that case, the sequences of the first group are called *proper* or *classic* Euler angles. (In this work, ***z-y-x*** is used)

3-2. Axis + angle

axis + angle is a single rotation by an angle θ_a about a vector e_a that runs through the fixed point. The vector itself does not perform rotations, but is used to construct transformations on vectors that correspond to rotations. The rotation occurs in the sense prescribed by the right-hand rule. The rotation axis is sometimes called the Euler axis.

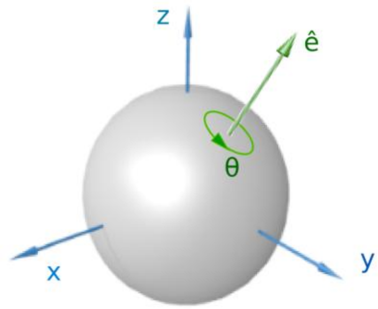

Figure 3-1: Axis + angle or Euler axis

3-3. Rotation matrix

A rotation matrix is a matrix that is used to perform a rotation in Euclidean space. In this case, orthogonal axes can be expressed as a matrix so that $C^T C = I$, $\det(C) = 1$. It means that a rotation matrix is an orthonormal matrix.

According to Figure 3-2, a rotation matrix is defined as

$$C = \begin{bmatrix} u_x & v_x & w_x \\ u_y & v_y & w_y \\ u_z & v_z & w_z \end{bmatrix} \tag{3-1}$$

Where u_x, u_y, u_z are the components of the unit vector **u** along the three axes of the reference orthogonal system (e.g. satellite centered inertial). In a similar way, v and w have components vectors **v** and **w** along the same reference axes [4].

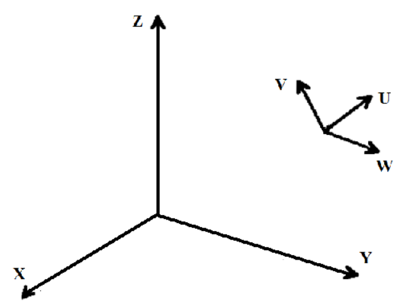

Figure 3-2: the orientation of the three axes U, V, W in the reference frame X, Y, Z

3-4. Quaternion

Quaternion is used for representing orientations and rotations of objects in three dimensions. Compared to Euler angle it avoids the problem of singularity. Compared to rotation matrix it is more compact.

The quaternion is defined as

$$\bar{\mathbf{q}} = q_0 + \mathbf{i}q_1 + \mathbf{j}q_2 + \mathbf{k}q_3 = q_0 + \boldsymbol{q} \tag{3-2}$$

Where q_0 is a scalar, $\boldsymbol{q}$ is defined as a vector part of the quaternion.

A rotation through an angle of θ_a around the axis defined by a unit vector e_a can be represented as [10]

$$\bar{\mathbf{q}} = \begin{bmatrix} \cos\frac{\theta_a}{2} \\ e_{a_x}\sin\frac{\theta_a}{2} \\ e_{a_y}\sin\frac{\theta_a}{2} \\ e_{a_z}\sin\frac{\theta_a}{2} \end{bmatrix} \tag{3-3}$$

It is clear that $\sum_{i=0}^{3} q_i^2 = 1$.

A quaternion rotation can be converted into a rotation matrix as [11]

$$C = \begin{bmatrix} q_0^2 + q_1^2 - q_2^2 - q_3^2 & 2(q_1q_2 + q_0q_3) & 2(q_1q_3 - q_0q_2) \\ 2(q_1q_2 - q_0q_3) & q_0^2 - q_1^2 + q_2^2 - q_3^2 & 2(q_2q_3 + q_0q_1) \\ 2(q_1q_3 + q_0q_2) & 2(q_2q_3 - q_0q_1) & q_0^2 - q_1^2 - q_2^2 + q_3^2 \end{bmatrix} \tag{3-4}$$

3-5. Euler Angles to Quaternion conversion

For converting Euler angles to quaternion, it is assumed z-y-x sequence. It means that first; the satellite rotates about z-axis then y-axis and finally rotates about x-axis. It can be represented as

$$\bar{\mathbf{q}} = \begin{bmatrix} \cos(\frac{\psi}{2}) \\ 0 \\ 0 \\ \sin(\frac{\psi}{2}) \end{bmatrix} \begin{bmatrix} \cos(\frac{\theta}{2}) \\ 0 \\ \sin(\frac{\theta}{2}) \\ 0 \end{bmatrix} \begin{bmatrix} \cos(\frac{\varphi}{2}) \\ \sin(\frac{\varphi}{2}) \\ 0 \\ 0 \end{bmatrix} \tag{3-5}$$

After doing simple calculations, eq. (3-5) can be written as

$$\begin{bmatrix} q_0 \\ q_1 \\ q_2 \\ q_3 \end{bmatrix} = \begin{bmatrix} (\cos\frac{\phi}{2}\ \cos\frac{\theta}{2}\ \cos\frac{\psi}{2}) + (\sin\frac{\phi}{2}\ \sin\frac{\theta}{2}\ \sin\frac{\psi}{2}) \\ (\sin\frac{\phi}{2}\ \cos\frac{\theta}{2}\ \cos\frac{\psi}{2}) - (\cos\frac{\phi}{2}\ \sin\frac{\theta}{2}\ \sin\frac{\psi}{2}) \\ (\cos\frac{\phi}{2}\ \sin\frac{\theta}{2}\ \cos\frac{\psi}{2}) + (\sin\frac{\phi}{2}\ \cos\frac{\theta}{2}\ \sin\frac{\psi}{2}) \\ (\cos\frac{\phi}{2}\ \cos\frac{\theta}{2}\ \sin\frac{\psi}{2}) - (\sin\frac{\phi}{2}\ \sin\frac{\theta}{2}\ \cos\frac{\psi}{2}) \end{bmatrix} \tag{3-6}$$

It is clear that other rotation sequences use different conventions [11].

3-6. Quaternion to Euler angles conversion

Converting quaternion to Euler angles can be obtained by the following equation [12]

$$\begin{bmatrix} \varphi \\ \theta \\ \psi \end{bmatrix} = \begin{bmatrix} \mathrm{atan}(\frac{2(q_0q_1 + q_2q_3)}{1-2(q_1^2+q_2^2)}) \\ \mathrm{a\,sin}(2(q_0q_2 - q_3q_1)) \\ \mathrm{atan}(\frac{2(q_0q_3 + q_1q_2)}{1-2(q_2^2+q_3^2)}) \end{bmatrix} \tag{3-7}$$

Note, however, that the atan and asin functions implemented in computer languages only produce results between −π/2 and π/2, and for three rotations between −π/2 and π/2 one does not obtain all possible orientations. To generate all the orientations, one needs to replace the atan functions in computer code by atan2.

$$\begin{bmatrix} \varphi \\ \theta \\ \psi \end{bmatrix} = \begin{bmatrix} \mathrm{atan2}(2(q_0q_1 + q_2q_3)\ ,\ (1-2(q_1^2+q_2^2))) \\ \mathrm{a\,sin}(2(q_0q_2 - q_3q_1)) \\ \mathrm{atan2}(2(q_0q_3 + q_1q_2)\ ,\ (1-2(q_2^2+q_3^2))) \end{bmatrix} \tag{3-8}$$

4. Satellite Kinematics and Dynamics

Dynamics and kinematics of a satellite are nonlinear models from Euler's moment equations. Attitude dynamic is the deferential equation describing how the angular velocities of the satellite change with the applied torques to the satellite. Attitude kinematic is the deferential equation describing how the attitude of the satellite changes with the angular velocities of the satellite.

4-1. Attitude dynamics

Attitude dynamics equation of satellite is obtained by Euler's moment equation [4].

$$\mathbf{T} = \frac{\mathrm{d}\mathbf{H}}{\mathrm{dt}} + \boldsymbol{\omega}_{\mathrm{bi}}^{\times}\ \mathbf{H} \tag{4-1}$$

Where **T** is the total external torques applied to the satellite, **H** is total angular momentum of the satellite, $\boldsymbol{\omega}_{bi}$ the angular velocity of the body-fixed reference with respect to the inertial frame and $\omega^{\times}$ denotes the skew symmetric matrix operator

$$\boldsymbol{\omega}^{\times} = \begin{bmatrix} 0 & -\omega_{\mathrm{bi}_z} & \omega_{\mathrm{bi}_y} \\ \omega_{\mathrm{bi}_z} & 0 & -\omega_{\mathrm{bi}_x} \\ -\omega_{\mathrm{bi}_y} & \omega_{\mathrm{bi}_x} & 0 \end{bmatrix} \tag{4-2}$$

For a rigid body, H is obtained as

$$\mathbf{H} = \mathbf{I_s}\ \boldsymbol{\omega}_{\mathrm{bi}} \tag{4-3}$$

Where $\mathbf{I_s}$ is the matrix of the inertia tensor of satellite. Therefore, Eq. (4-1) can be represented as

$$\mathbf{T_c} + \mathbf{T_d} = \mathbf{I_s}\frac{\mathrm{d}\boldsymbol{\omega}_{\mathrm{bi}}}{\mathrm{dt}} + \boldsymbol{\omega}_{\mathrm{bi}}^{\times}\ \mathbf{I_s}\boldsymbol{\omega}_{\mathrm{bi}} \tag{4-4}$$

Where $\mathbf{T_d}$ is the external disturbance torque and $\mathbf{T_c}$ is the control torque generated by controller. Eq.(4-4) can be written as

$$\frac{\mathrm{d}\boldsymbol{\omega}_{\mathrm{bi}}}{\mathrm{dt}} = -\mathbf{I_s}^{-1}\boldsymbol{\omega}_{\mathrm{bi}}^{\times}\ \mathbf{I_s}\boldsymbol{\omega}_{\mathrm{bi}} + \mathbf{I_s}^{-1}\mathbf{T_c} + \mathbf{I_s}^{-1}\mathbf{T_d} \tag{4-5}$$

4-2. Attitude kinematics

The kinematic equations of motion are a set of first-order differential equations specifying the time evolution of the attitude parameters (Euler angles, quaternion, and rotation matrix). These equations contain the instantaneous angular velocity vector [9]. In this work, quaternion parameterization is considered.

Let the quaternion $\bar{\mathbf{q}}$ represent the orientation of the rigid body with respect to the reference system at time t ($\bar{\mathbf{q}} = [q_0 \quad q_1 \quad q_2 \quad q_3]^T$), and $\bar{\mathbf{q}}''$ represent the orientation with respect to the reference system at time (t+Δt). Then $\bar{\mathbf{q}}'$ specifies the orientation at time (t+Δt) relative to the position that it occupied at time t:

$$\bar{\mathbf{q}}' = \begin{bmatrix} \cos\frac{\Delta\theta_a}{2} \\ e_{a_x}\ \sin\frac{\Delta\theta_a}{2} \\ e_{a_y}\ \sin\frac{\Delta\theta_a}{2} \\ e_{a_z}\ \sin\frac{\Delta\theta_a}{2} \end{bmatrix} \tag{4-6}$$

Where e_{ax}, e_{ay}, e_{az} are the elements of the rotation axis unit vector at time t and $\Delta\theta_a$ is the rotation angle in time (Δt). Therefore

$$\bar{\mathbf{q}}'' = A(\bar{\mathbf{q}}')\,\bar{\mathbf{q}} \tag{4-7}$$

Where $\bar{\mathbf{q}}'' = \bar{\mathbf{q}}(t+\Delta t)$, $\bar{\mathbf{q}} = \bar{\mathbf{q}}(t)$ and $A(\bar{\mathbf{q}}')$ is defined as

$$A(\bar{\mathbf{q}}') = \left[\cos\frac{\Delta\theta_a}{2} I + \sin\frac{\Delta\theta_a}{2}\begin{bmatrix} 0 & e_{a_z} & -e_{a_y} & e_{a_x} \\ -e_{a_z} & 0 & e_{a_x} & e_{a_y} \\ e_{a_y} & -e_{a_x} & 0 & e_{a_z} \\ -e_{a_1} & -e_{a_2} & -e_{a_3} & 0 \end{bmatrix}\right] \tag{4-8}$$

Where **I** is a unit matrix 4×4. Eq.(4-8) could be converted to a differential equation. In this case, Δt is infinitesimal and $\Delta\theta_a = \omega_{bi}\Delta t$. For small angle approximations

$$\cos\frac{\Delta\theta_a}{2} \approx 1,\ \sin\frac{\Delta\theta_a}{2} \approx \frac{1}{2}\omega_{bi}\ \Delta t \tag{4-9}$$

and

$$\bar{\mathbf{q}}(t+\Delta t) = [I + \frac{1}{2}\Omega\ \Delta t]\bar{\mathbf{q}}(t) \tag{4-10}$$

Where Ω is the skew symmetric matrix of the angular velocity vector ($\boldsymbol{\omega}_{bi}$). Then

$$\frac{\bar{\mathbf{q}}(t+\Delta t) - \bar{\mathbf{q}}(t)}{\Delta t} = \frac{1}{2}\Omega\ \bar{\mathbf{q}}(t) \tag{4-11}$$

If $\Delta t \rightarrow 0$, then

$$\frac{d}{dt}\bar{\mathbf{q}}(t) = \frac{1}{2}\Omega\ \bar{\mathbf{q}}(t) \tag{4-12}$$

5. Attitude Actuators

5-1. Magnetorquer

These actuators are used to generate a controllable magnetic moment for attitude control. The magnetic moment is generated when an electrical current is passed through its coil. It is given by

$$M = I_M . N . A \tag{5-1}$$

Where N is the number of coils, A is the cross-sectional area that the coils encompass, and I_M is the input current of the magnetorquer. In this work, it is assumed that N = 200, A = 49E-4.

Interaction between the magnetic moment and the earth's magnetic field produces a mechanical torque to control the satellite. This torque is shown as [4]

$$T_M = M \times B \tag{5-2}$$

Where **M** is the bipolar magnetic produced in the satellite, **B** is the Earth's magnetic field intensity with respect to the body coordinates.

According to Eq.(5-2)

1) T_M is zero when B is parallel to M ($B \parallel M \rightarrow T_M = 0$).
2) T_M is the maximum achievable when B is perpendicular to M ($B \perp M \rightarrow T_M : \max$).

A sample of this actuator is shown in Figure 5-1.

Figure 5-1**:** A sample of magnetorquer [13]

Advantages of this actuator are as follows [14, 15]

- Simplicity
- Reliability
- Lightweight
- Low Volume
- Low Power Consumption
- Simple Operation

Disadvantages of this actuator are as follows [14, 15]

- Low Level of Torque
- Dependence on Earth's Magnetic Field Strength
- No Torque along Earth's Magnetic Field
- Difficult beyond LEO

5-2. Reaction Wheel

Reaction Wheel (RW) is one of the most common momentum exchange devices used for attitude control [4]. When an electrical current is applied to RW, the torque of this actuator is generated as

$$T_w = K_M I_w \tag{5-3}$$

This actuator has its own angular momentum.

$$\mathbf{h}_w = I_w \boldsymbol{\omega}_w + I_w \mathbf{D}\boldsymbol{\omega}_{bi} \tag{5-4}$$

Where $\mathbf{h}_w$ is angular momentum of the wheel, I_w is the inertia momentum of reaction wheel, **D** is the wheel orientation matrix that shows which wheels are mounted on which axis. The torque of each wheel on the body of the satellite along the fixed-body coordinate axis is expressed by $\dot{h}_w$ that is equal to the negative torque of this wheel on the satellite body.

$$\frac{d\mathbf{h}_w}{dt} = -\mathbf{T} \tag{5-5}$$

Therefore

$$\mathbf{T} = -\frac{d\mathbf{h}_w}{dt} = -I_w \dot{\omega}_w - I_w D \dot{\omega}_{bi} \tag{5-6}$$

Eq. (5-6) can be rewritten as follows

$$I_w \dot{\omega}_w = -T_w - I_w D \dot{\omega}_{bi} \tag{5-7}$$

Also, attitude dynamics equation of satellite with reaction wheel actuators is rewritten as [16]

$$\frac{d\boldsymbol{\omega}_{bi}}{dt} = -\mathbf{I}_s^{-1} \boldsymbol{\omega}_{bi}^{\times} \mathbf{I}_s \boldsymbol{\omega}_{bi} + \mathbf{I}_s^{-1} \mathbf{T}_c + \mathbf{I}_s^{-1} \mathbf{T}_d \tag{5-8}$$

$$(\mathbf{I}_S - D\,\mathbf{I}_W)\dot{\omega}_{bi} = -\omega_{bi}^{\times} (\mathbf{I}_S \omega_{bi} + D\,\mathbf{I}_W \omega_W) + DT_w + \mathbf{d} \tag{5-9}$$

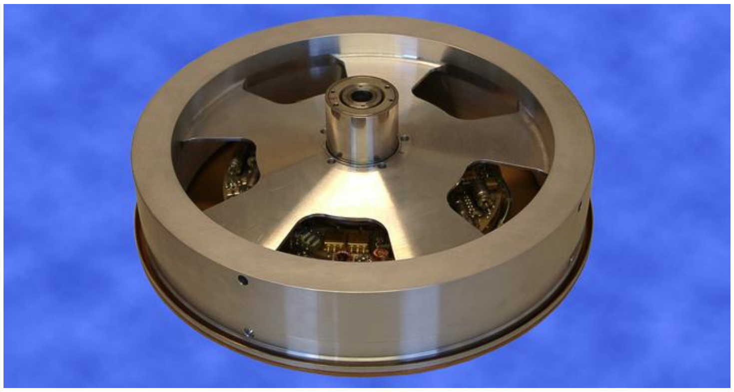

Figure 5-2**:** a sample of reaction wheel [17]

Where **d** is the external disturbance torque and T_w is the control torque generated by reaction wheel.

A sample of this actuator is shown in Figure 5-2.

Advantages of this actuator, in comparison with magnetorquer, are as follows [4]

- High Level of Torque
- High Accuracy of Attitude Tracking
- Independence on Earth's Magnetic Field Strength
- Minimum Parasitic Torque Disturbances

6. Attitude Control

The attitude of a satellite is its orientation in the body fixed coordinate frame with respect to a frame reference.

Satellite attitude control is controlling the orientation in the given direction. It requires actuators to apply the torques needed to re-orient the satellite to a given attitude [15].

The various algorithms are used to command the actuators, such as robust, optimal linear, nonlinear control and etc.

In this work, Sliding Mode Control method is utilized that is a nonlinear control.

6-1. Sliding Mode Control

If the tasks of a control system involve large range and/or high speed motions, nonlinear effects will be significant in the dynamics and nonlinear control may be necessary to achieve the desired performance. In modeling most systems due to non-modeling dynamics and possible nonlinear effects in the linearization of system equations, and also disturbance and noise, there may be uncertainties. To control these systems, SMC[1] theory can be used. It is one of the robust and nonlinear control methods for uncertain systems [18].

SMC design provides a systematic approach to the problem of maintaining stability and performance in the face of modeling imprecision.

The main concepts and notations of SMC and the associated basic controller designs are explained in the following.

Consider the following dynamic system [18]

$$x^{(n)}(t) = f(x) + g(x)u(t) \tag{6-1}$$

Where u(t) is control signal, x(t) is state variable, f(x) and g(x) are nonlinear functions, they may also have an uncertain part with upper bound that is known continues function. The control

[1] sliding mode control

problem is to get the state vector $\mathbf{x}=\begin{bmatrix} x & \dot{x} & \dots & x^{(n-1)} \end{bmatrix}$ to track a specific time-varying state $\mathbf{x_d}=\begin{bmatrix} x_d & \dot{x}_d & \dots & x_d^{(n-1)} \end{bmatrix}$ in the presence of model imprecision on f(x) and g(x). Suppose a designed control law constraints the motion of the system to the following sliding surface (S(x,t)=0)

$$s(\mathbf{x},t)=\left(\frac{d}{dt}+\lambda\right)^{n-1}\tilde{\mathbf{x}} \tag{6-2}$$

Where λ is a positive constant and $\tilde{\mathbf{x}}$ is

$$\tilde{\mathbf{x}}=\mathbf{x}-\mathbf{x}_d \tag{6-3}$$

As mentioned, the purpose of control is to stabilize the sliding surface and converge it to zero. For this purpose, the Lyapunov stability theory is used. So, the Lyapunov function candidate is selected as follow.

$$v=\frac{1}{2}S^2 \tag{6-4}$$

Where v is a positive define function. According to the theory of the stability of Lyapunov, if the derivative of a function is negative define function ($\dot{v}<0$), then the function will be asymptotic stability. But in SMC theory to guarantee finite time convergence of sliding variable, the sliding condition should be satisfied.

$$\dot{v}=S(t)\dot{S}(t)\le-\eta|S(t)| \tag{6-5}$$

Where η is a positive constant. The time duration of convergence is obtained by integrating sliding condition inequality (6-5) as following.

$$\int_{S(0)}^{0}\frac{S(t)}{|S(t)|}\,dS\le\int_{0}^{t_r}-\eta\,dt \tag{6-6}$$

After doing the math operations,

$$t_r\le\frac{S(0)}{\eta} \tag{6-7}$$

Where t_r can be changed by changing η. By substituting eq. (6-2) into eq. (6-5),

$$S\left(\frac{d^{(n)}\tilde{\mathbf{x}}}{dt}+\cdots+\lambda^n\tilde{\mathbf{x}}\right)\le-\eta|S(t)| \tag{6-8}$$

By substituting eq. (6-1) and eq. (6-3) into eq.(6-8), the following eq. is obtained

$$S\left(f(x)+g(x)u(t)-\mathbf{x}_d^{(n)}+\cdots+\lambda^n(\mathbf{x}-\mathbf{x}_d)\right)\le-\eta|S(t)| \tag{6-9}$$

The control signal u(t) should be selected so that the inequality (6-9) is satisfied. The signal control consists of a *reaching phase* and a *sliding phase*. In *reaching phase*, the trajectories start off the manifold S = 0 move toward it and reach it in finite time, followed by a *sliding phase* during which the motion is confined to the manifold S = 0 [16]. These phases are illustrated in Figure 6-1 [18].

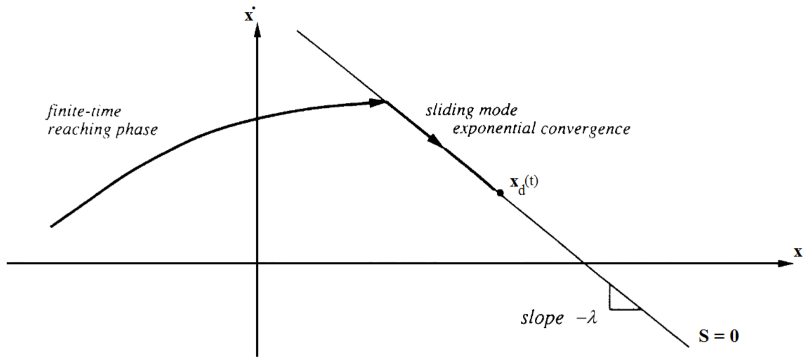

Figure 6-1**:** Graphical interpretation of equations (2) and (5), (n=2) [18]

As mentioned, the control signal should be satisfied sliding condition. It is selected as following

$$u = u_{eq} - k\ \mathrm{sgn}(S) \tag{6-10}$$

Where sgn(S) = 0 for S = 0, k = μ+β, β is the upper bound of uncertain part of f(x), u_{eq} is designed to remove certain items in eq. (6-9). In the following equation, it should be noted that only certain part of f(x) is considered.

$$u_{eq} = g^{-1}(x)\left(-f(x) + x_d^{(n)} + \cdots - \lambda(\mathbf{x} - \mathbf{x}_d)\right) \tag{6-11}$$

For more information, please refer to [18, 19]. In the following, advantages and disadvantages of SMC are explained.

Advantages:

Some advantages of SMC are [18, 20]:

- disturbance rejection
- insensitivity to parameter variations
- maintaining stability in the presence of uncertainty
- Order reduction
- decoupling design procedures,

Disadvantages:

Main disadvantage of SMC is the phenomenon of chattering. It is due to the sign function (sgn(S)) and consists of sudden and rapid variation of the control signal [21]. Chattering is undesirable in practice, since it involves high control activity and further may excite high-frequency dynamics neglected in the course of modeling (such as unmodeled structural modes, neglected time-delays, and so on) [18]. The phenomenon chattering is shown in Figure 6-2.

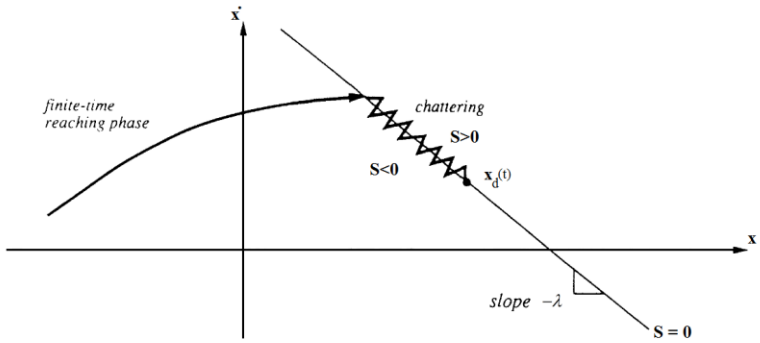

Figure 6-2**:** Chattering as a result of imperfect control switching modified [18]

Sliding control has been successfully applied to robot manipulators, underwater and aerospace vehicles, vehicle and motion control, process control, automotive transmissions and engines, high-performance electric motors, generators and power systems [18, 20].

In the following section, satellite attitude control by using SMC is described.

6-2. SMC design for satellite attitude control

In this work, the control objectives are to achieve an attitude tracking in the presence of external disturbance. For this, SMC method is utilized.

To design SMC, at first, the error signal is defined. The error signal is $e_{\bar{q}} = \bar{\mathbf{q}}_d - \bar{\mathbf{q}}$, $\bar{\mathbf{q}}$ is the quaternion and $\bar{\mathbf{q}}_d$ is the desired quaternion. Sliding surface is defined as

$$s = e_{\bar{q}}^{\bullet} + k e_{\bar{q}} \qquad \textbf{(6-12)}$$

To make the sliding variable asymptotically converge to zero, the control rule must satisfy the sliding mode condition ($s^T s^{\bullet} < 0$). Deviating (6-12) and substituting (4-12) is given

$$s^{\bullet} = e_{\bar{q}}^{\bullet\bullet} + k e_{\bar{q}}^{\bullet} = (\bar{\mathbf{q}}^{\bullet\bullet} - \bar{\mathbf{q}}_d^{\bullet\bullet}) + k e_{\bar{q}}^{\bullet} = k e_{\bar{q}}^{\bullet} - \bar{\mathbf{q}}_d^{\bullet\bullet} + \frac{1}{2}(\Omega^{\bullet}\bar{\mathbf{q}} + \Omega\bar{\mathbf{q}}^{\bullet}) \qquad \textbf{(6-13)}$$

Where $\Omega^{\bullet}\bar{\mathbf{q}}$ is rewritten as

$$\Omega^{\bullet}\bar{\mathbf{q}} = \begin{bmatrix} -q_1 & -q_2 & -q_3 \\ q_0 & -q_3 & q_2 \\ q_3 & q_0 & -q_1 \\ -q_2 & q_1 & q_0 \end{bmatrix} \begin{bmatrix} \omega_1^{\bullet} \\ \omega_2^{\bullet} \\ \omega_3^{\bullet} \end{bmatrix} = \bar{Q}\,\omega_{bi}^{\bullet} \qquad \textbf{(6-14)}$$

Expression $\Omega\bar{\mathbf{q}}^{\bullet}$, is given as

$$\Omega\bar{\mathbf{q}}^{\bullet} = \frac{1}{2}\Omega(\frac{1}{2}\Omega\bar{\mathbf{q}}) = -\frac{1}{4}(\omega_{bi_x}^2 + \omega_{bi_y}^2 + \omega_{bi_z}^2)\bar{\mathbf{q}} \tag{6-15}$$

By substituting (4-4) into (6-14), (6-13) is obtained as follows

$$\dot{s} = k e_{\bar{q}}^{\bullet} - \bar{\mathbf{q}}_d^{\bullet\bullet} - \frac{1}{4}(\omega_{bi_x}^2 + \omega_{bi_y}^2 + \omega_{bi_z}^2)\bar{\mathbf{q}} - \frac{1}{2}\bar{Q}\mathbf{I}_s^{-1}\omega_{bi}^{\times}\mathbf{I_s}\omega_{bi} + \frac{1}{2}\bar{Q}\,\mathbf{I}_s^{-1}T_c \tag{6-16}$$

The control signal should be designed in such a way to satisfy the sliding condition. In SMC method, the control signal is chosen as $u = u_{eq} + u_r$, where u_{eq} is used to remove the effect of the definite expression from the first derivative of the sliding variable and u_r is used to eliminate the effect of the indeterminate. These expressions are shown in (6-17) and (6-18) respectively.

$$u_{eq} = -2\mathbf{I_s}\bar{Q}^{-1}[k e_{\bar{q}}^{\bullet} - \bar{\mathbf{q}}_d^{\bullet\bullet} - \frac{1}{4}(\omega_{bi_x}^2 + \omega_{bi_y}^2 + \omega_{bi_z}^2)\bar{\mathbf{q}} - \frac{1}{2}\bar{Q}\mathbf{I}_s^{-1}\omega_{bi}^{\times}\mathbf{I_s}\omega_{bi}] \tag{6-17}$$

$$u_r = -2\mathbf{I_s}\bar{Q}^{-1}K\,\mathrm{sgn}(s) \tag{6-18}$$

Where $K \in \mathbb{R}^3$ is design variable vector.

6-2-1. Satellite attitude control with magnetorquer actuator

The control signal is a desired torque applied on the satellite. So, the actuators have to generate a magnetic moment that interaction between this magnetic moment and the earth's magnetic field produces this desired mechanical torque to control the satellite. Therefore, the desired torque generated by controller should be converted to the desired magnetic moment of the magnetorquer then the input current of the magnetorquer must be obtained.

At first, it is assumed that there is one magnetorquer mounted on X-axis. So, eq. (5-2) can be written as

$$\begin{bmatrix} T_{magx} \\ T_{magy} \\ T_{magz} \end{bmatrix} = \begin{bmatrix} 0 & b_z & -b_y \\ -b_z & 0 & -b_x \\ b_y & -b_x & 0 \end{bmatrix} \begin{bmatrix} M_x \\ 0 \\ 0 \end{bmatrix} = \begin{bmatrix} 0 \\ -b_z M_x \\ b_y M_x \end{bmatrix} \tag{6-19}$$

As mentioned, for a desired torque, to be applied on the satellite, the magnetic moment vector must be generated. In this case, M_x can be obtained as

$$M_x = \frac{1}{b_z^2 + b_y^2}\begin{bmatrix} 0 & -b_z & b_y \end{bmatrix} T_c \tag{6-20}$$

Where b_z and b_y are the magnetic field of the earth in the body frame coordinates with respect to inertia frame coordinates.

Then, it is assumed that there are two magnetorquers mounted on the X-axis and Z-axis. So, eq. (5-2) can be written as

$$\begin{bmatrix} T_{magx} \\ T_{magy} \\ T_{magz} \end{bmatrix} = \begin{bmatrix} 0 & b_z & -b_y \\ -b_z & 0 & -b_x \\ b_y & -b_x & 0 \end{bmatrix} \begin{bmatrix} M_x \\ 0 \\ M_z \end{bmatrix} = \begin{bmatrix} -b_y M_z \\ -b_z M_x - b_x M_z \\ b_y M_x \end{bmatrix} \tag{6-21}$$

Therefore, M_x can be obtained as eq. (6-20) and M_z can be obtained as

$$M_z = \frac{1}{b_x^2 + b_y^2} \begin{bmatrix} -b_y & -b_x & 0 \end{bmatrix} T_c \tag{6-22}$$

Where b_x, b_y and b_z are the magnetic field of the earth in the body frame coordinates with respect to inertia frame coordinates.

In the other example, it is assumed that three magnetorquers mounted on each axis are used. In this case, M vector can be obtained as

$$\mathrm{M} = \frac{\mathrm{B(b)^T}}{|\mathrm{b}|^2} \mathrm{Tc} \tag{6-23}$$

Where T_c is desired control torque produced by controller, b is the Earth's magnetic field intensity with respect to the body coordinates and B(b) matrix is explained by Eq. (5-2). The inverse of B(b) isn't used because this matrix is singular.

Now, the input current of the magnetorquer for generating the desired magnetic moment must be obtained as

$$I_{M_i} = \frac{M_i}{N.A} \tag{6-24}$$

Where M_i is magnetic moment generated by magnetorquer mounted on i axis and I_{Mi} is the input current of the magnetorquer mounted on i axis.

6-2-2. Satellite attitude control with reaction wheel actuator

As mentioned, attitude dynamics equation of satellite with reaction wheel actuators is obtained by eq. (5-9). Therefore, by substituting (5-9) into (6-14), (6-16) is rewritten as follows

$$\dot{\mathrm{s}} = \mathrm{k}\dot{\mathrm{e}}_{\bar{\mathrm{q}}} - \ddot{\bar{\mathbf{q}}}_{\mathrm{d}} - \frac{1}{4}(\omega_{\mathrm{bi_x}}^2 + \omega_{\mathrm{bi_y}}^2 + \omega_{\mathrm{bi_z}}^2)\bar{\mathbf{q}} - \frac{1}{2}\bar{\mathrm{Q}}\mathbf{I}_{\mathrm{s}}^{-1}\omega_{\mathrm{bi}}^{\times}\mathbf{I}_{\mathbf{s}}\omega_{\mathrm{bi}} - \frac{1}{2}\bar{\mathrm{Q}}\mathbf{I}_{\mathrm{s}}^{-1}\omega_{\mathrm{bi}}^{\times}\mathrm{DI}_{\mathrm{w}}\omega_{\mathrm{w}} + \frac{1}{2}\bar{\mathrm{Q}}\,\mathbf{I}_{\mathrm{s}}^{-1}\mathrm{T_c} \tag{6-25}$$

So, u_{eq} is rewritten as following

$$u_{eq} = -2\mathbf{I}_{\mathbf{s}}\bar{Q}^{-1}[k\dot{e}_{\bar{q}} - \ddot{\bar{\mathbf{q}}}_{d} - \frac{1}{4}(\omega_{bi_x}^2 + \omega_{bi_y}^2 + \omega_{bi_z}^2)\bar{\mathbf{q}} - \frac{1}{2}\bar{Q}\,\mathbf{I}_s^{-1}\omega_{bi}^{\times}\mathbf{I}_{\mathbf{s}}\omega_{bi} - \frac{1}{2}\bar{Q}\,\mathbf{I}_s^{-1}\omega_{bi}^{\times}DI_w\omega_w] \tag{6-26}$$

In this case, u_r is the same as eq. (6-18).

7. Simulation examples

In this section, the proposed attitude control is simulated for the nanosatellites with several combinations of the actuators. At first, a sample attribute motion for tracking has been described. Then, attitude dynamic and kinematic of the satellite has been explained. The numerical model for the attitude control has been described in the next section. Finally, the performed simulations are explained.

7-1. Desired Motion

The desired angle of the each axis of the satellite can be represented as follows [22]

$$\gamma(t) = \gamma_0 + \frac{T_{max}}{\mathbf{I}_s} \int_{t_0}^{t} \int_{t_0}^{\tau_1} f(\Delta t, t_f, \tau_2)\, d\tau_2\, d\tau_1 \tag{7-1}$$

Where γ_0 is initial angle, T_{max} is maximum available torque, $\mathbf{I}_s$ is the momentum inertia element, t_0 is initial time, τ_1 and τ_2 are symbols for integrating variables and f(.) is an approximation of the signum function that is given as

$$f(\Delta t, t_f, \tau_2) = \begin{cases} (\frac{t}{\Delta t})\left(3 - 2(\frac{t}{\Delta t})\right) & 0 \le t \le \Delta t \\ 1 & \Delta t \le t \le t_1 \\ 1 + (\frac{t - t_1}{\Delta t})\left(3 - 2(\frac{t - t_2}{2\Delta t})\right) & t_1 \le t \le t_2 \\ -1 & t_2 \le t \le t_3 \\ -1 + (\frac{t - t_3}{\Delta t})\left(3 - 2(\frac{t - t_3}{\Delta t})\right) & t_3 \le t \le t_f \end{cases} \tag{7-2}$$

Where $t_1 = \frac{t_f}{2} - \Delta t$, $t_2 = \frac{t_f}{2} + \Delta t$, $t_3 = t_f - \Delta t$ and t_f is a final time.

As mentioned, quaternion describes the attitude orientation of the satellite in this work. Euler angles to quaternion conversion are obtained by eq. (3-6).

7-2. The numerical model of the satellite

To simplify, the fixed parameters of the systems are written in a “m.file” that can be modified at any time. These parameters are defined as

```
Is =eye(3)*0.012;          %the matrix of the inertia tensor of the satellite
t_final = 300;             %final time for each desired angles
Euler_d = [60;45;0];       %final desired angles [deg] - first z, then y, then x
initial_Euler = [0;0;0];   %initial euler angles [deg]
```

Where Is is the symmetric positive definite moment inertia matrix of the cube satellite, `t_final` is final time, `Euler_d` is final desired angle vector, `initial_Euler` is initial euler angle vector.

7-3. Describing simulation satellite attitude models

To verify the performance of the proposed controller, numerical simulations are performed. At first, the presented equations are used as the models of the satellite in MATLAB. They are shown in Figure 7-1.

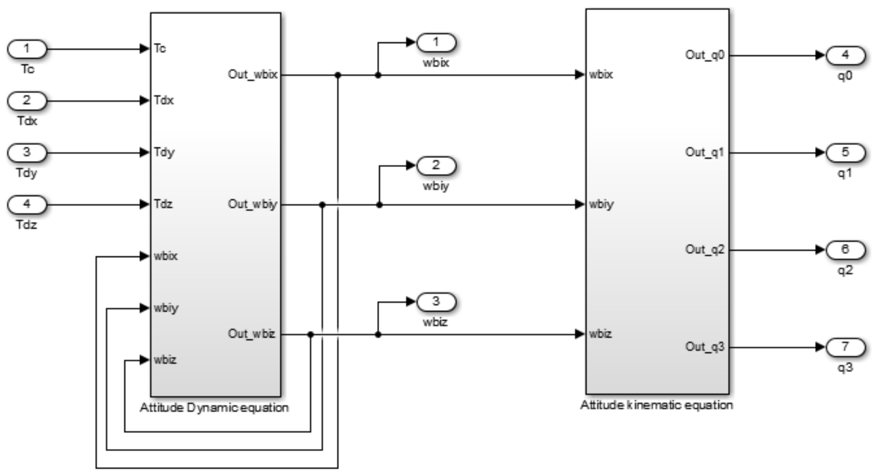

Figure 7-1: Attitude Dynamic and Kinematic Models

Where $[q_0, q_1, q_2, q_3]$ are quaternion, $[\omega_{bix}, \omega_{biy}, \omega_{biz}]$ are the angular velocities of the body-fixed reference with respect to the inertial frame, $\mathbf{T_c}$ is the control torque produced by the actuators and T_{dx}, T_{dy}, T_{dz} are the disturbance torques.

The satellite's dynamics and kinematics details are shown in Figure 7-2 and Figure 7-3, respectively.

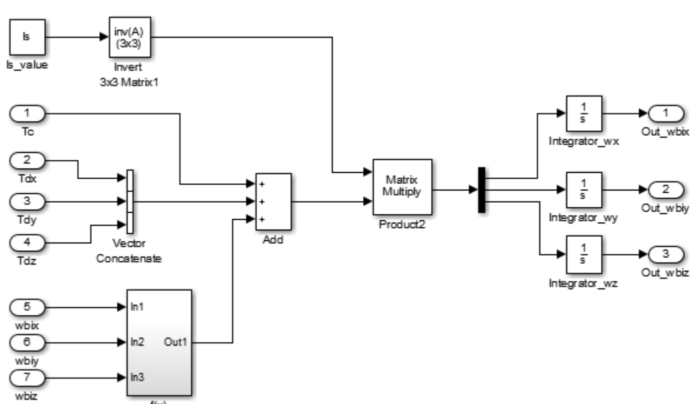

Figure 7-2: Satellite Attitude Dynamic

Where f(x) is given as

```
function y = fcn(wx,wy,wz,Is,Iw,D,Ww)

ww = [0 -wz wy;
      wz 0 -wx;
      -wy wx 0];
y = - inv(Is) * ww * ((Is * [wx;wy;wz]);
```

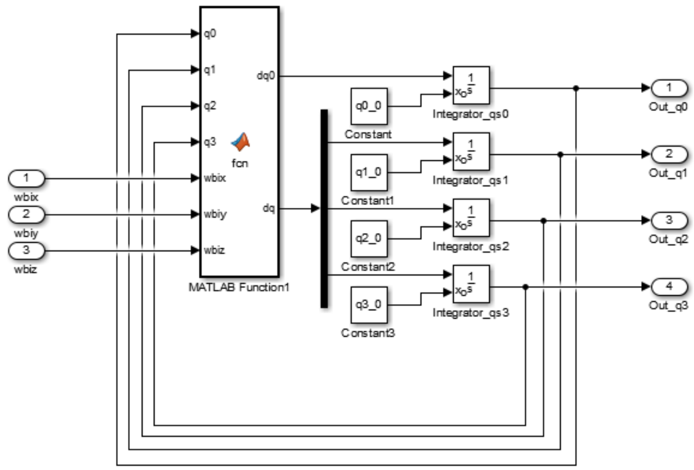

Figure 7-3: Satellite Attitude Kinematic

Where (q0_0, q1_0, q2_0, q3_0) are the initial values of quaternion converted from initial Euler angles by eq. (6) and g(x) is given as

```
function [dq0,dq] = fcn(q0,q1,q2,q3,wbix,wbiy,wbiz)

q = [q1;q2;q3];
skew_symmetric_matrix_qs = [0 -q3 q2;
                            q3 0 -q1;
                            -q2 q1 0];
dq0 = -0.5*qs'*[wbix;wbiy;wbiz];
dq = 0.5*((q0*eye(3))+skew_symmetric_matrix_qs)*[wbix;wbiy;wbiz];
```

7-4. Describing actuator model

The magnetorquer model is shown in Figure 7-4.

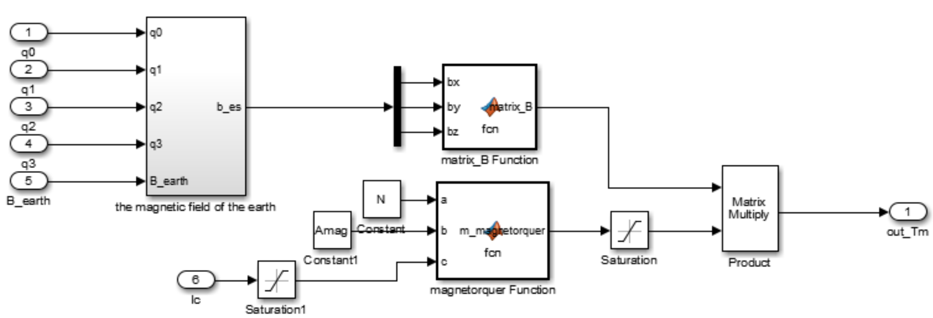

Figure 7-4: magnetorquer model

Where I_c is the input current of the actuators generated by controller, the saturation block is used to limit the input current, B_es is the earth of magnetic field with respect to Body frame coordinates that is obtained from the following equation

$$B\_es = C^{-1} * B\_earth \qquad \textbf{(7-3)}$$

Where B_earth vector is obtained by eq. (2-4) and C is rotation matrix defined as

$$C = \begin{bmatrix} q_0^2+q_1^2-q_2^2-q_3^2 & 2(q_1q_2+q_0q_3) & 2(q_1q_3-q_0q_2) \\ 2(q_1q_2-q_0q_3) & q_0^2-q_1^2+q_2^2-q_3^2 & 2(q_2q_3+q_0q_1) \\ 2(q_1q_3+q_0q_2) & 2(q_2q_3-q_0q_1) & q_0^2-q_1^2-q_2^2+q_3^2 \end{bmatrix} \qquad \textbf{(7-4)}$$

Also, matrix_B is defined as

$$matrix\_B = \begin{bmatrix} 0 & b_z & -b_y \\ -b_z & 0 & b_x \\ b_y & -b_x & 0 \end{bmatrix} \qquad \textbf{(7-5)}$$

Where b_x, b_y, b_z are the elements vector of the earth of magnetic field is obtained by Eq. (2-4).

The magnetorquer parameters are defined as

```
N = 200;            %number of coils
Amag = 49E-4;       %cross-sectional area
Imax = 0.5;         %maximum current
```

Where *N* is the number of magnetorquer coils, *Amag* is the cross-sectional area that the coils encompass and I_{max} is the maximum current passing through the coils.
The reaction wheel model is shown in Figure 7-5.

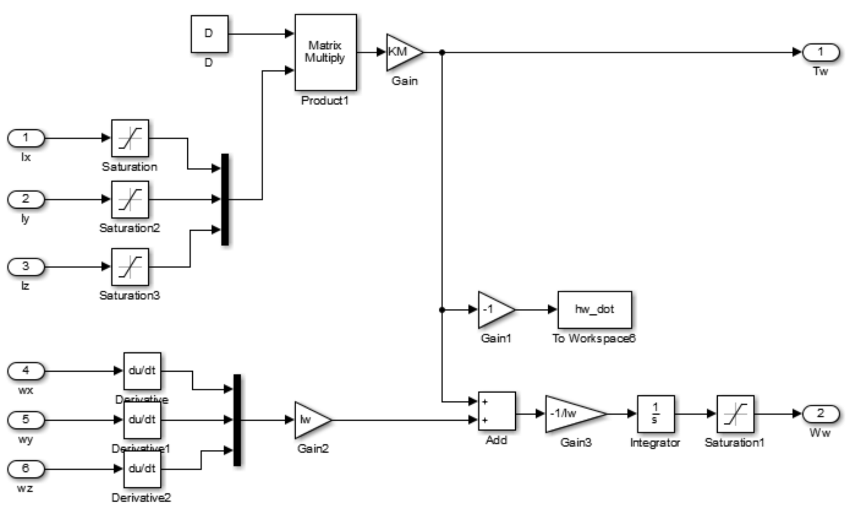

Figure 7-5: Reaction Wheel model

Where I_x, I_y, I_z are the input current of the actuators generated by controller, the saturation block is used to limit the input current, K_M is the torque coefficient and $T_w = I_{RW}\ K_M$ where T_w is the torque produced by the motor [4].

Reaction wheel parameters are defined as

```
Iw = 50e-6;
D = [1 0 0;
     0 1 0;
     0 0 1];
KM = 9.5e-3;          %[Nm/A] torque constant
Imax = 0.5;           %[A]
Wmax = 40;            %[red/sec]
```

Where Iw is the inertia of the reaction wheel, D is the wheel distribution matrix, K_M is the torque coefficient in the reaction wheel, Imax is the maximum current that could be applied to the reaction wheel, Wmax is the maximum angular velocity of the reaction wheel.

As mentioned, Attitude dynamics equation of satellite by using Reaction Wheel actuator is defined by Eq. (5-9). It is shown in Figure 7-6.

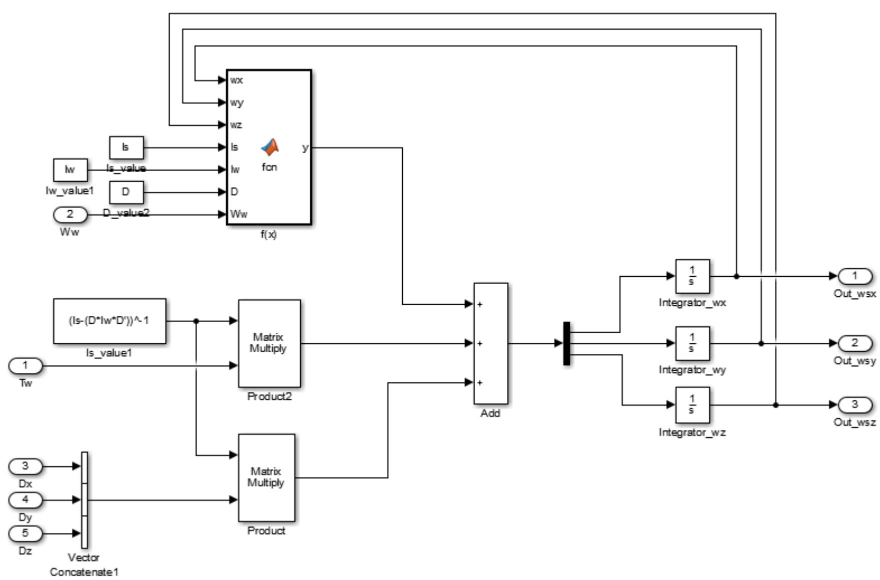

Figure 7-6: Modified Attitude Dynamic satellite with Reaction Wheels

Where f(x) is given as

```
function y = fcn(wx,wy,wz,Is,Iw,D,Ww)
ww = [0 -wz wy;
      wz 0 -wx;
      -wy wx 0];
y = - inv(Is-(D*Iw*D')) * ww * ((Is * [wx;wy;wz]) + (Iw*D*Ww));
```

7-5. Simulations

In this work, it is assumed that the satellite is located in a circular orbit with following characteristics

```
Rearth = 6971E3;
w0 = 0.0011;
i = 0;
Mag_earth = 7.96E15;
G = 6.674E-11;
```

Where Rearth is distance from the center of the earth, Mag_earth is the earth's magnetic constant, i is inclination, w0 is the orbital rotation frequency that is defined as $\sqrt{\frac{G.Mearth}{\text{Rearth}^3}}$, G is gravitational constant.

7.5.1. Simulation results by one magnetorquer

In this section, the performance of proposed controller is presented to the satellite attitude control by one magnetorquer mounted on X-axis. The simulation results are shown the following figures.

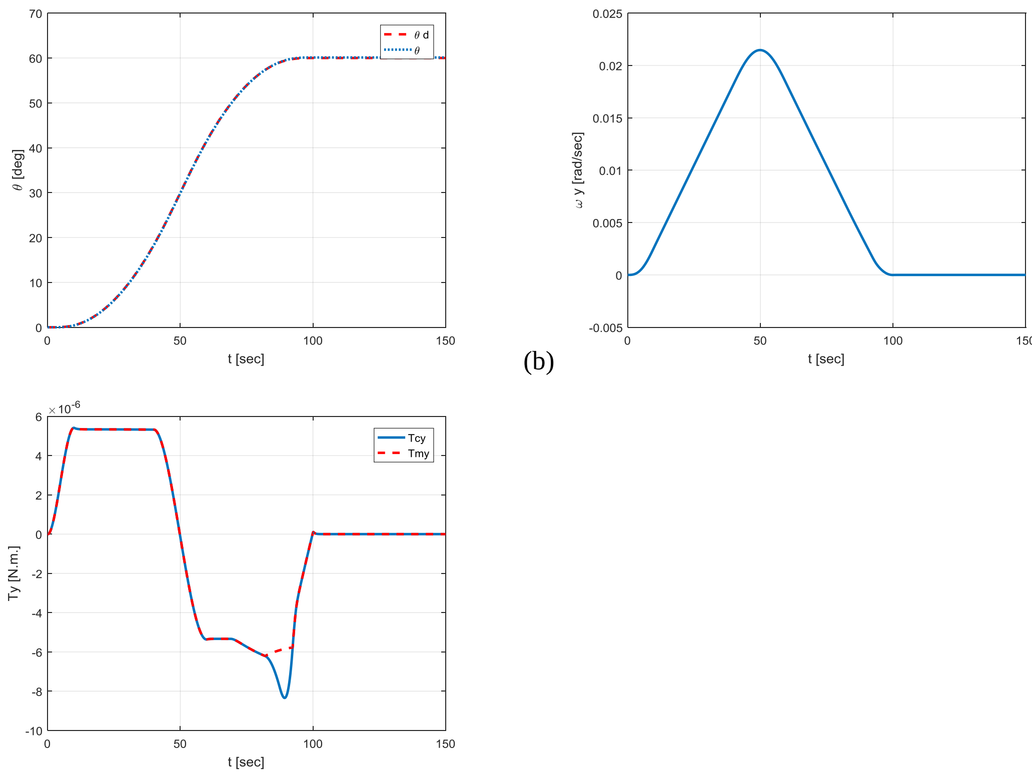

(a) (b) (c)

Figure 7-7: (a) desired angle and rotation angle about Y-axis (θ), (b) angular velocity, (c) input control torque and torque generated in the satellite

As shown in Figure 7-7, the system rotates 60 degrees around y-axis and it could track the desired angle, the angular velocity converges to zero and the torque generated in the satellite is in the limitation range.

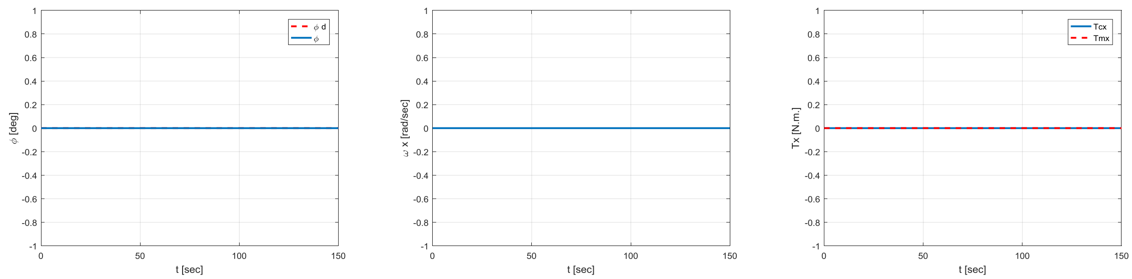

(a) (b) (c)

Figure 7-8**:** desired angle and rotation angle about X-axis (φ), (b) angular velocity, (c) input control torque and torque generated in the satellite

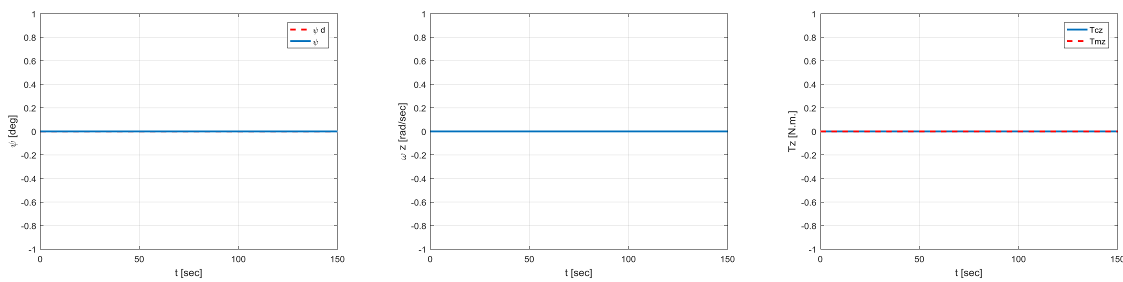

(a) (b) (c)

Figure 7-9**:** (a) desired angle and rotation angle about Z-axis (ψ), (b) angular velocity, (c) input control torque and torque generated in the satellite

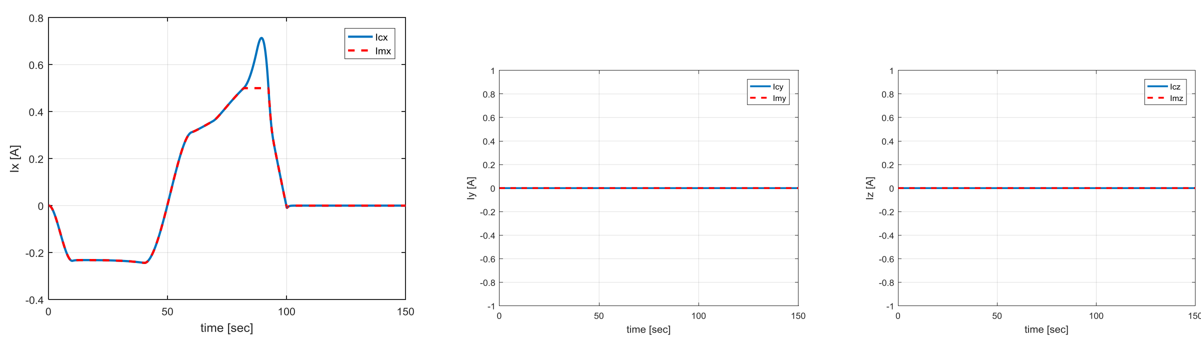

(a) (b) (c)

Figure 7-10**:** the magnetorquer currents laid on the (a) X-axis, (b) Y-axis and (c) Z-axis

As shown in Figure 7-8 and Figure 7-9, angular velocity and rotation angle around X-axis and Z-axis are zero and the controller doesn't generate any torque in X-axis and Z-axis. Magnetorquer current laid on the Y-axis and Z-axis are zero because there are no magnetorquers on these axes.

As shown in Figure 7-10, the magnetorquer currents laid on the Y-axis and Z-axis are zero and the magnetorquer current laid on the Y-axis is in the limitation range and converges to zero.

In the next simulation, the desired angle is 180 degrees around y-axis. It means that the satellite rotates 180 degrees around y-axis. As shown in Figure 7-11, the satellite can rotate and track the desired angle, the angular velocity converges to zero and the torque generated in the satellite is in the limitation range.

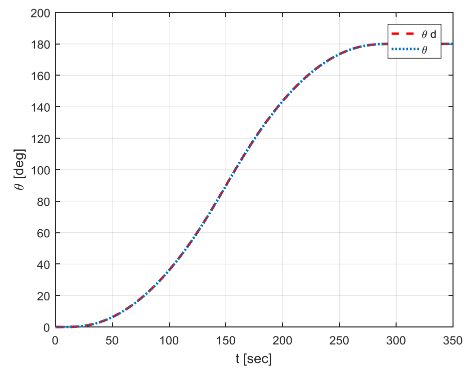

(a)

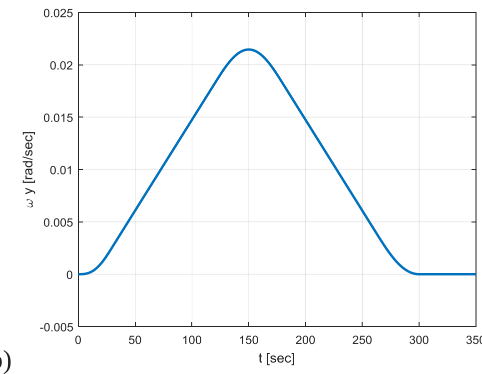

(b)

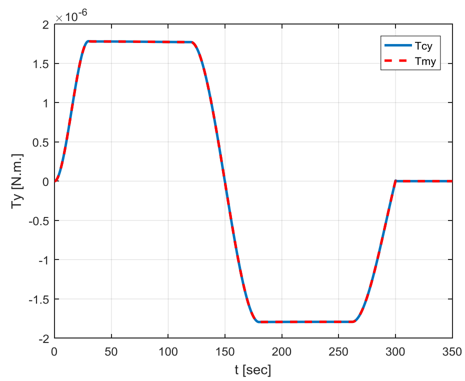

(c)

Figure 7-11**:** (a) desired angle and rotation angle about Y-axis (θ), (b) angular velocity, (c) input control torque and torque generated in the satellite

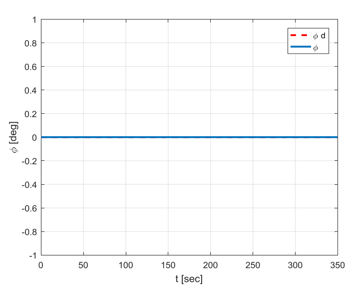

(a)

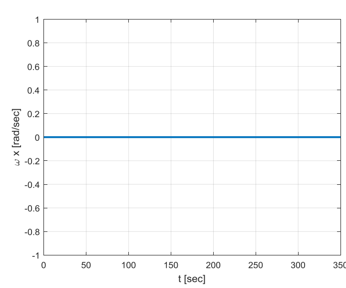

(b)

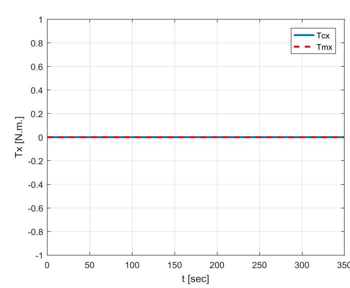

(c)

Figure 7-12**:** (a) desired angle and rotation angle about X-axis (φ), (b) angular velocity, (c) input control torque and torque generated in the satellite

As shown in Figure 7-12 and Figure 7-13, angular velocity and rotation angle around X-axis and Z-axis are zero and the controller doesn't generate any torque in X-axis and Z-axis. Magnetorquer current laid on the Y-axis and Z-axis are zero because there are no magnetorquers on these axes. As shown in Figure 7-14, the magnetorquer currents laid on the Y-axis and Z-axis are zero and the magnetorquer current laid on the Y-axis is in the limitation range and converges to zero. But, the amplitude of the current generated by the controller is large at 150 seconds. At this time, the magnetic field of the earth and the actuator are aligned so no torque is generated. For solving this problem, two magnetorquers are used.

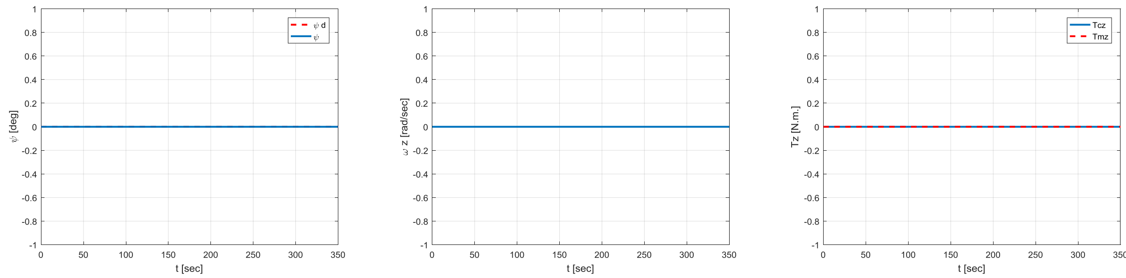

(a) (b) (c)

Figure 7-13**:** (a) desired angle and rotation angle about Z-axis (ψ), (b) angular velocity, (c) input control torque and torque generated in the satellite

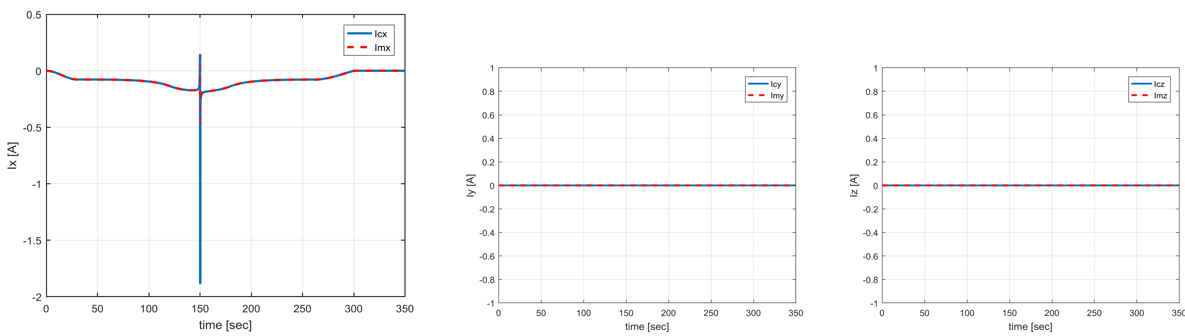

(a) (b) (c)

Figure 7-14**:** the magnetorquer currents laid on the (a) X-axis, (b) Y-axis, (c) Z-axis

7.5.2. Simulation results by two magnetorquers

In this section, two magnetorquers laid on the X-axis and Z-axis are used. At a moment, a magnetorquer is used that is produced the highest efficiency. As long as the angle between the actuator and the magnetic field of the earth is more than 45 degrees, this actuator is used; otherwise, another actuator is used to generate the torque.

As shown in Figure 7-15, the system rotates 90 degrees around y-axis and it could track the desired angle, the angular velocity converges to zero and the torque generated in the satellite is in the limitation range.

As shown in Figure 7-16 and Figure 7-17, angular velocity and rotation angle around X-axis and Z-axis are zero and the controller doesn't generate any torque in X-axis and Z-axis. Magnetorquer current laid on the Y-axis is zero because there is no magnetorquer on this axis.

As shown in Figure 7-18, the magnetorquer current laid on the Y-axis is zero and the magnetorquer currents laid on the X-axis and Z-axis are in the limitation range and converges to zero.

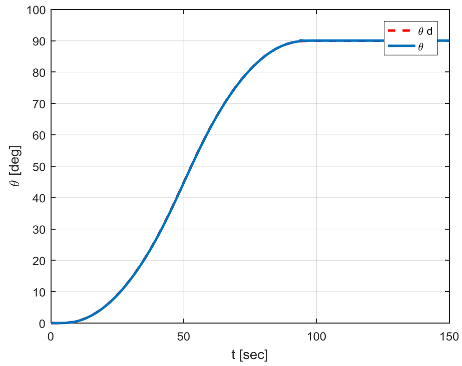

(a)

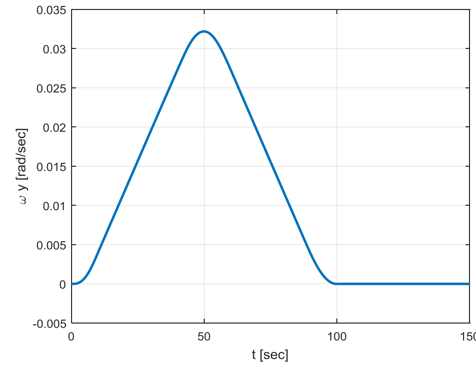

(b)

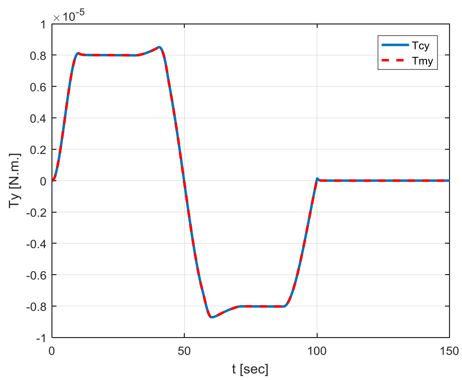

(c)

Figure 7-15**:** (a) desired angle and rotation angle about Y-axis (θ), (b) angular velocity, (c) input control torque and torque generated in the satellite

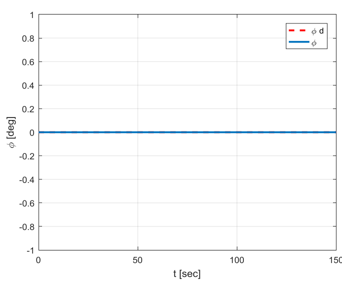

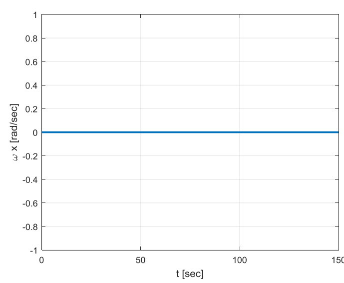

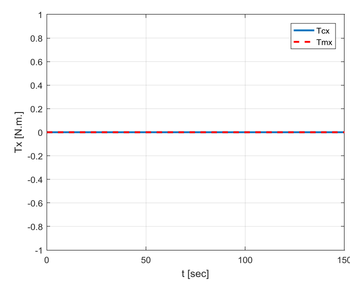

(a) (b) (c)

Figure 7-16**:** (a) desired angle and rotation angle about X-axis (φ), (b) angular velocity, (c) input control torque and torque generated in the satellite

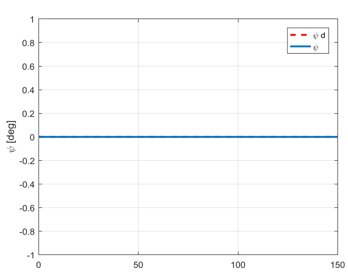

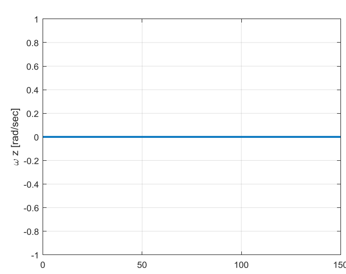

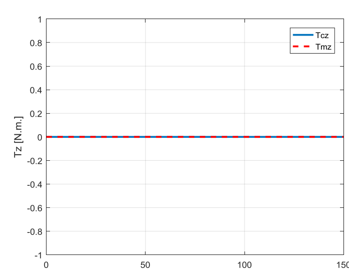

(a) (b) (c)

Figure 7-17**:** (a) desired angle and rotation angle about Z-axis (ψ), (b) angular velocity, (c) input control torque and torque generated in the satellite

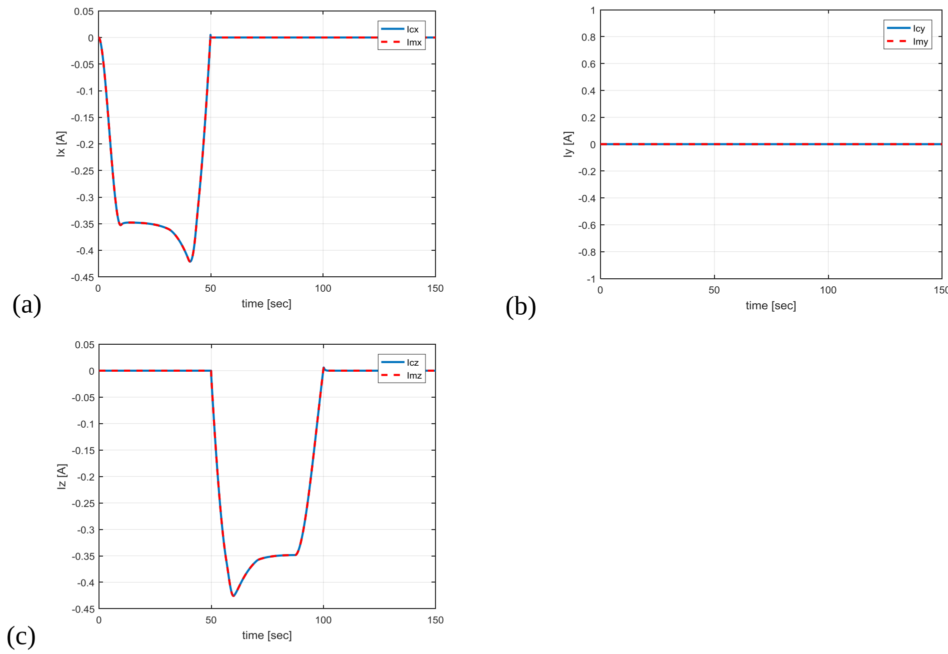

Figure 7-18**:** the magnetorquer currents laid on the (a) X-axis, (b) Y-axis, (c) Z-axis

In the next simulation, the desired angle is 180 degrees around y-axis. It means that the satellite rotates 180 degrees around y-axis. As shown in Figure 7-19, the satellite can rotate and track the desired angle, the angular velocity converges to zero and the torque generated in the satellite is in the limitation range.

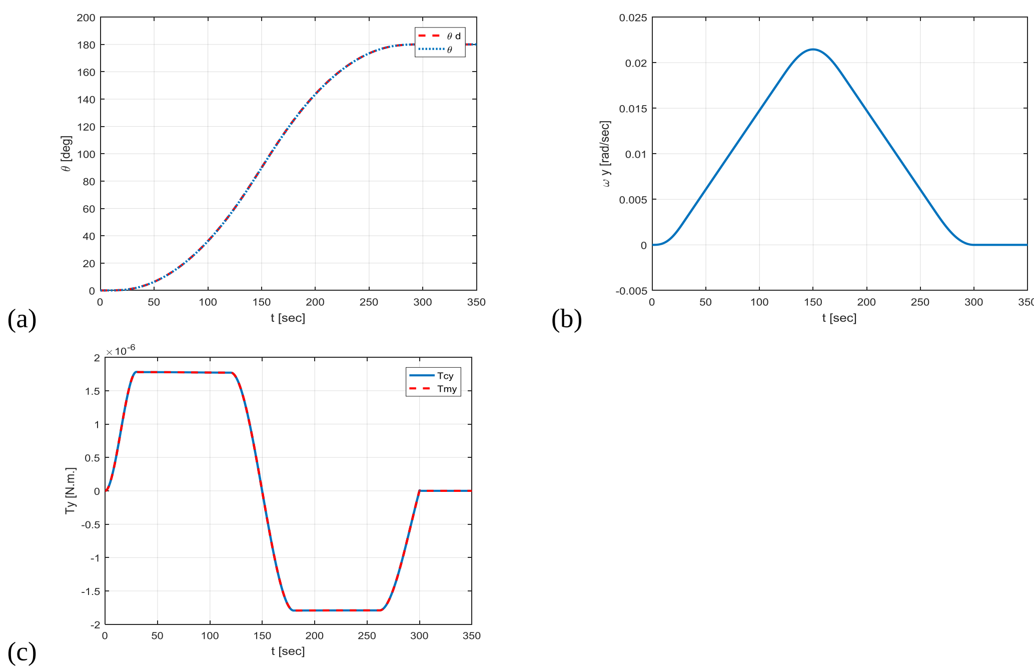

Figure 7-19**:** (a) desired angle and rotation angle about Y-axis (θ), (b) angular velocity, (c) input control torque and torque generated in the satellite

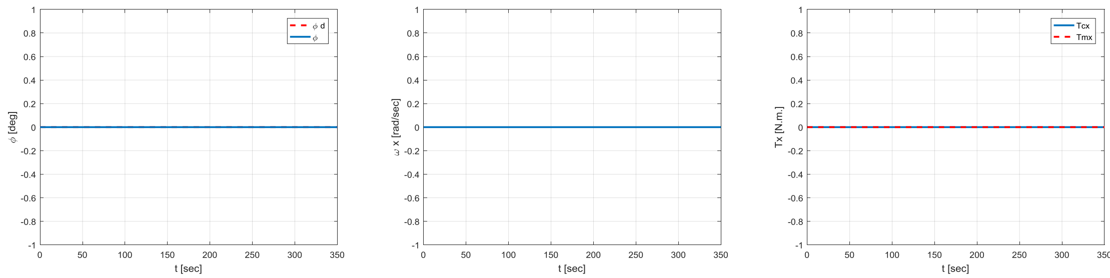

(a) (b) (c)

Figure 7-20**:** (a) desired angle and rotation angle about X-axis (φ), (b) angular velocity, (c) input control torque and torque generated in the satellite

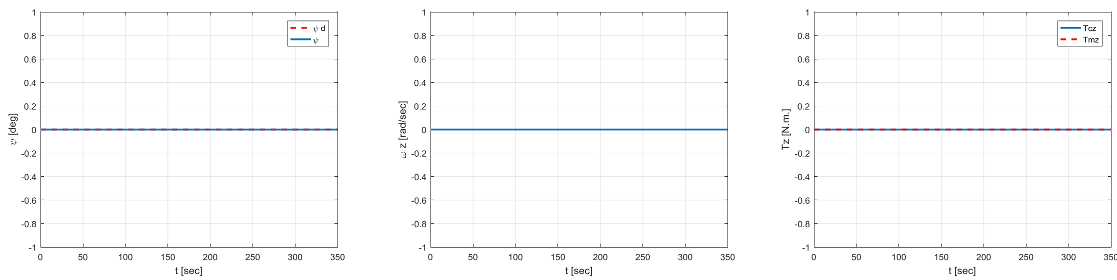

(a) (b) (c)

Figure 7-21**:** (a) desired angle and rotation angle about Z-axis (ψ), (b) angular velocity, (c) input control torque and torque generated in the satellite

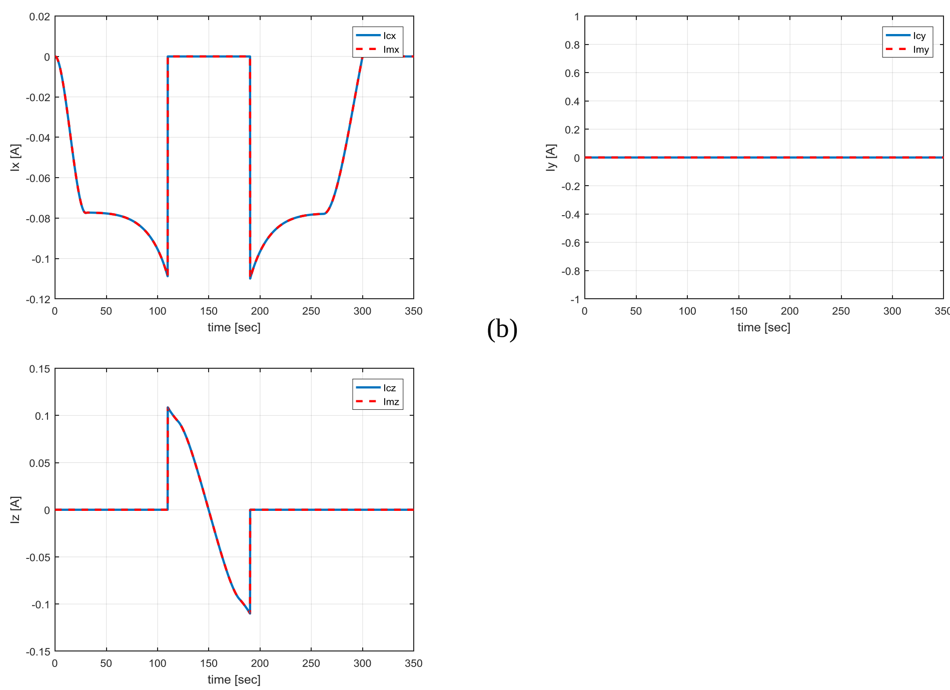

(a) (b) (c)

Figure 7-22**:** the magnetorquer currents laid on the (a) X-axis, (b) Y-axis, (c) Z-axis

As shown in Figure 7-20 and Figure 7-21, angular velocity and rotation angle around X-axis and Z-axis are zero and the controller doesn't generate any torque in X-axis and Z-axis.

Magnetorquer current laid on the Y-axis is zero because there is no magnetorquer on this axis.

As shown in Figure 7-22, the magnetorquer current laid on the Y-axis is zero and the magnetorquer currents laid on the X-axis and Z-axis are in the limitation range and converge to zero. Contrary to the system control with one magnetorquer, in this case the current amplitudes of the magnetorquers do not suddenly increase; because, the magnetic field of the earth and the actuators are not aligned.

7.5.3. Simulation results by one Reaction Wheel

The proposed controller is capable of tracking any desired angles. The desired angles can be obtained by (7-2) or changed during the simulation. For this situation, manual switch, slider gain and constant blocks are used as shown in Figure 7-23.

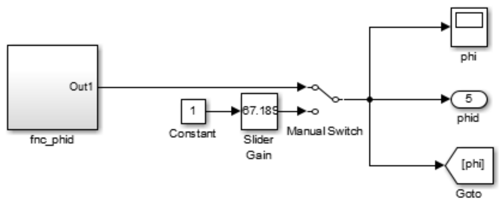

Figure 7-23**:** desired angle

As shown in Figure 7-24, the desired angle can be manually changed. To do this, double click on the menu button and use the slider gain block to select the desired angle. Minimum and maximum value can be defined manually and with moving the slider, the value of the desired angle can be changed.

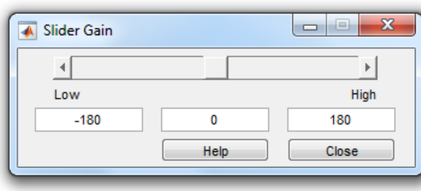

Figure 7-24**:** Slider Gain

As shown in Figure 7-24, -180, 0, 180 are minimum, current and maximum values, respectively. In order to observe the angular changes and the results obtained from them, some settings on the scope block and the simulation time should be changed. For example, the simulation time should be set to “inf”. For changing some settings on the scope block, it is necessary to go to view> configuration properties> Time and change “Time span overrun action” to scroll and “Time span” to 1000 or any values preferred.

In this section, the performance of proposed controller is presented to the satellite attitude control by one reaction wheel mounted on Y-axis. In this case, the wheel distribution matrix is defined as

$$D = \begin{bmatrix} 0 & 0 & 0 \\ 0 & 1 & 0 \\ 0 & 0 & 0 \end{bmatrix} \quad \textbf{(7-6)}$$

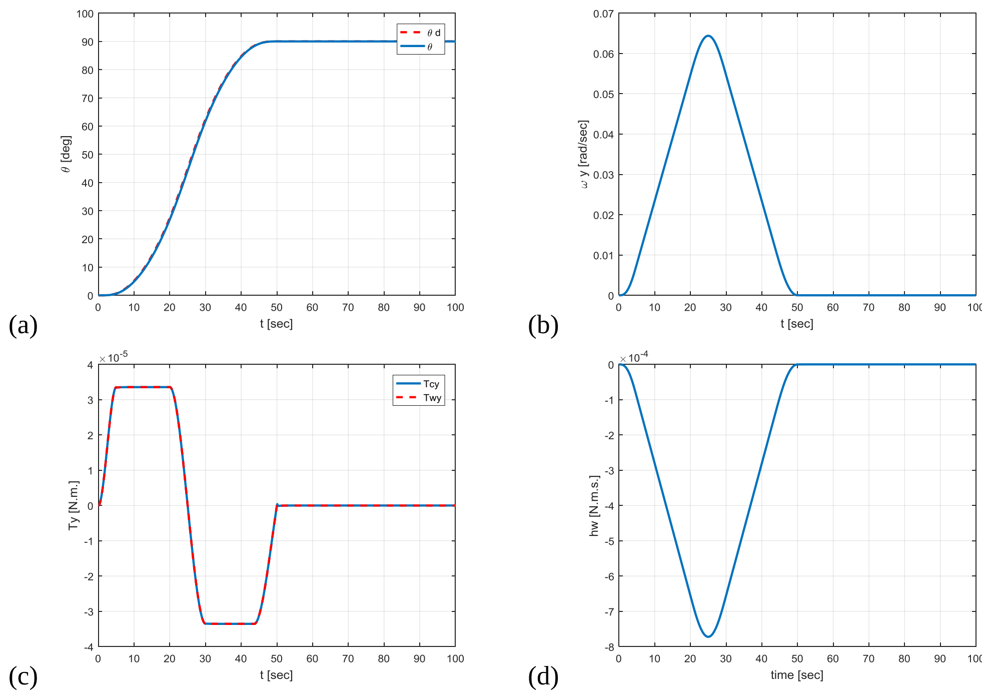

Figure 7-25**:** (a) desired angle and rotation angle about Y-axis (θ), (b) angular velocity, (c) input control torque and reaction wheel torque, (d) reaction wheel momentum

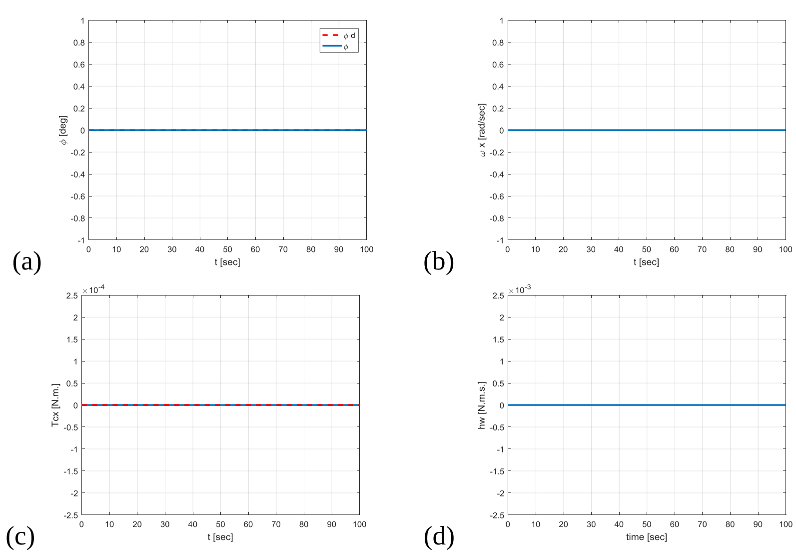

Figure 7-26**:** (a) desired angle and rotation angle about X-axis (φ), (b) angular velocity, (c) input control torque and reaction wheel torque, (d) reaction wheel momentum

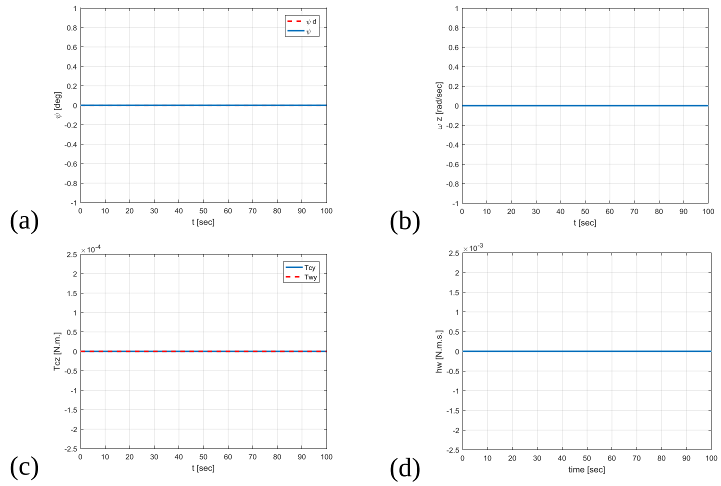

Figure 7-27: (a) desired angle and rotation angle about Z-axis (ψ), (b) angular velocity, (c) input control torque and reaction wheel torque, (d) reaction wheel momentum

As shown in Figure 7-25, the system rotates 90 degrees around y-axis and it could track the desired angle, the angular velocity converges to zero, reaction wheel torque and momentum is in the limitation range. As shown in Figure 7-26 and Figure 7-27, angular velocity, reaction wheel torque and momentum and rotation angle around x-axis and z-axis are zero and the controller doesn't generate any torque in x-axis and z-axis.

In the next simulation, desired angle is changed during the simulation.

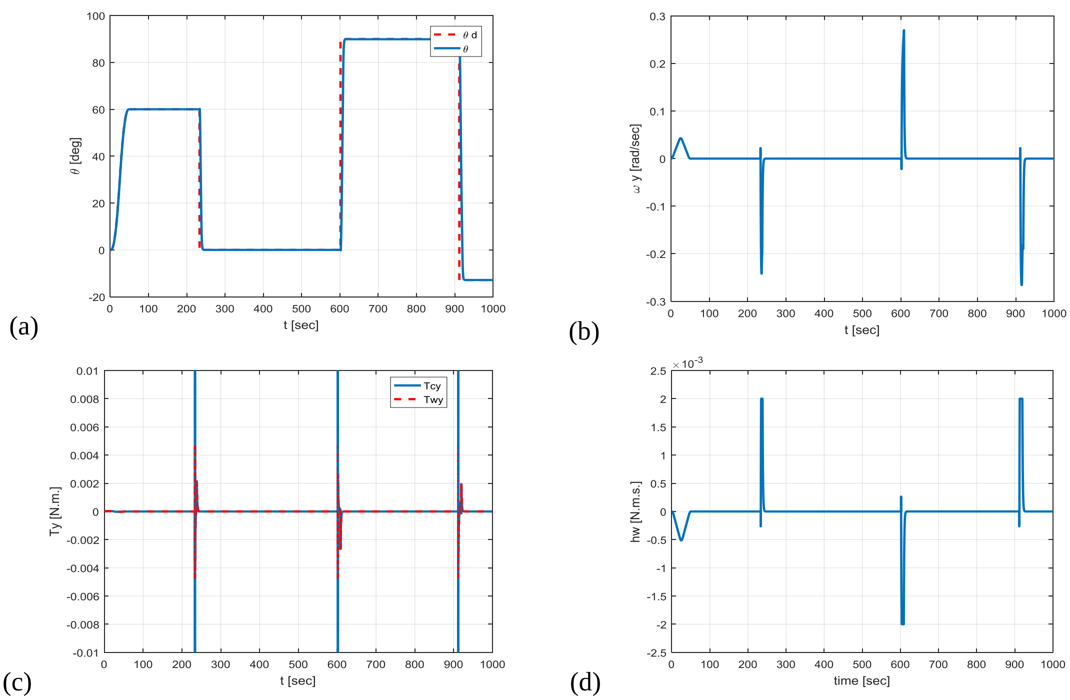

Figure 7-28: (a) desired angle and rotation angle about Y-axis (θ), (b) angular velocity, (c) input control torque and reaction wheel torque, (d) reaction wheel momentum

The simulation results are shown in Figure 7-28. It can be seen from results that, the proposed controller can generate a control signal so that system can track the desired angle. Also, the amplitude of the reaction wheel torque and momentum is in the limitation range.

7.5.4. Simulation results by three reaction wheels

In this section, the performance of proposed controller is presented to the satellite attitude control by three reaction wheels mounted on each main axis and the satellite can rotate around each of the three axes. In this case, the wheel distribution matrix is defined as

$$D = \begin{bmatrix} 1 & 0 & 0 \\ 0 & 1 & 0 \\ 0 & 0 & 1 \end{bmatrix} \tag{7-7}$$

The proposed controller performance is investigated for [60, 45, 90] rotations around z, y, x axis, respectively. In this case, the reaction wheel constraints are considered. Simulation results are shown in Figure 7-29, Figure 7-30 and Figure 7-31.

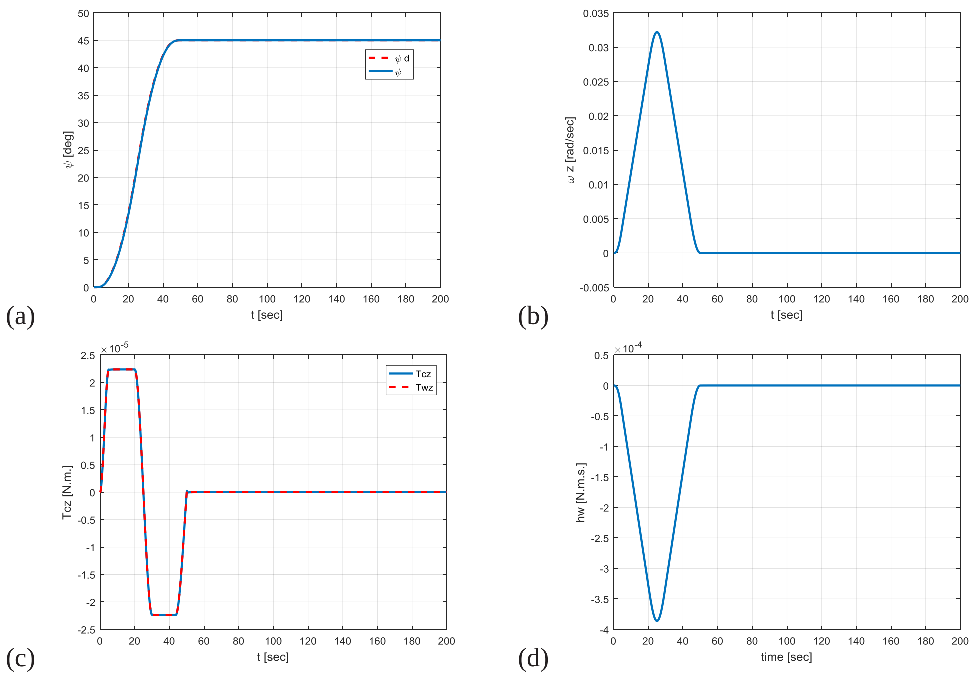

Figure 7-29**:** (a) desired angle and rotation angle about Z-axis (ψ), (b) angular velocity, (c) input control torque and reaction wheel torque, (d) reaction wheel momentum

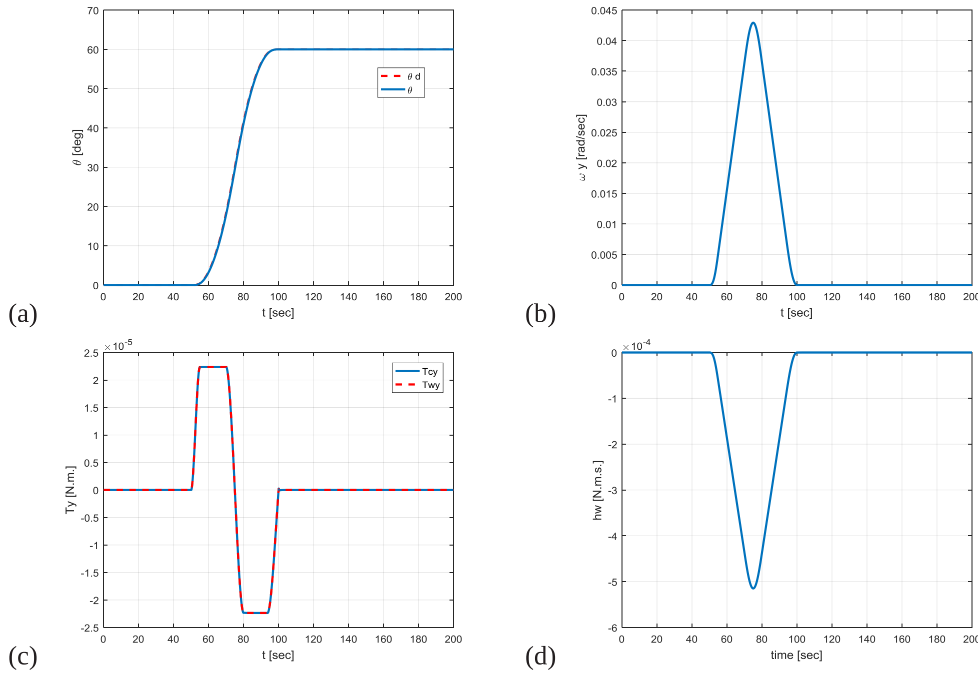

Figure 7-30**:** (a) desired angle and rotation angle about Y-axis (θ), (b) angular velocity, (c) input control torque and reaction wheel torque, (d) reaction wheel momentum

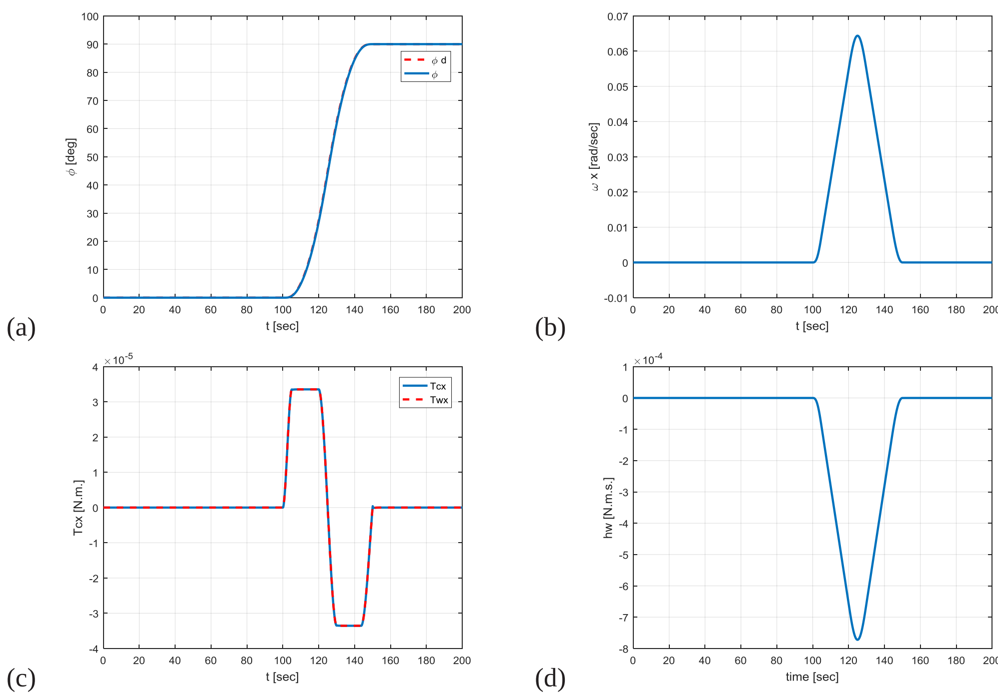

Figure 7-31**:** (a) desired angle and rotation angle about X-axis (φ), (b) angular velocity, (c) input control torque and reaction wheel torque, (d) reaction wheel momentum

In the next simulation, the desired rotations are chosen [120, -80, 180] degrees about Z, Y and X axes, respectively. Rotation time for each axis is chosen 50 seconds.

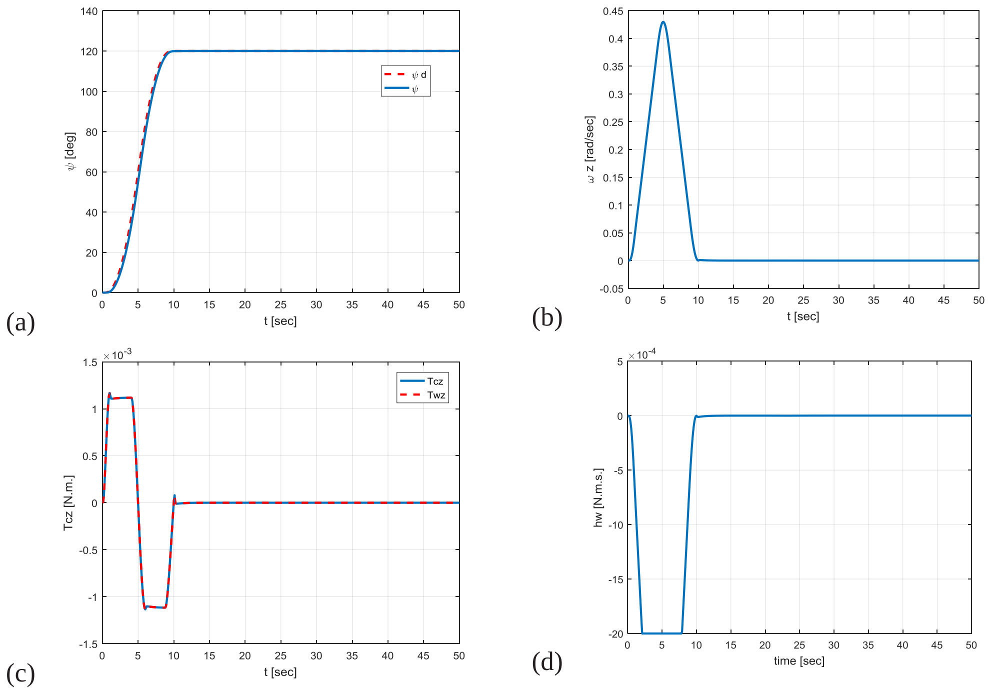

Figure 7-32**:** (a) desired angle and rotation angle about Z-axis (ψ), (b) angular velocity, (c) input control torque and reaction wheel torque, (d) reaction wheel momentum

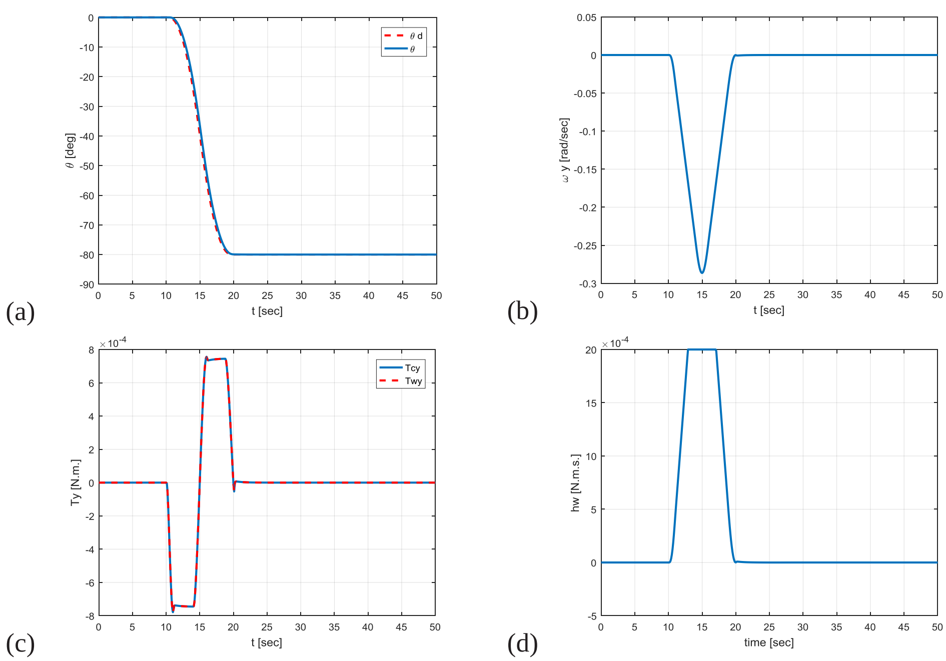

Figure 7-33**:** (a) desired angle and rotation angle about Y-axis (θ), (b) angular velocity, (c) input control torque and reaction wheel torque, (d) reaction wheel momentum

It can be seen from Figure 7-32–Figure 7-34 (a) that the Euler angles follow the desired angles very well. As shown in Figure 7-32–Figure 7-34(b), the angular velocities can converge to zero. It can be seen from Figure 7-32–Figure 7-34 (c, d) that actuator input constraints are considered.

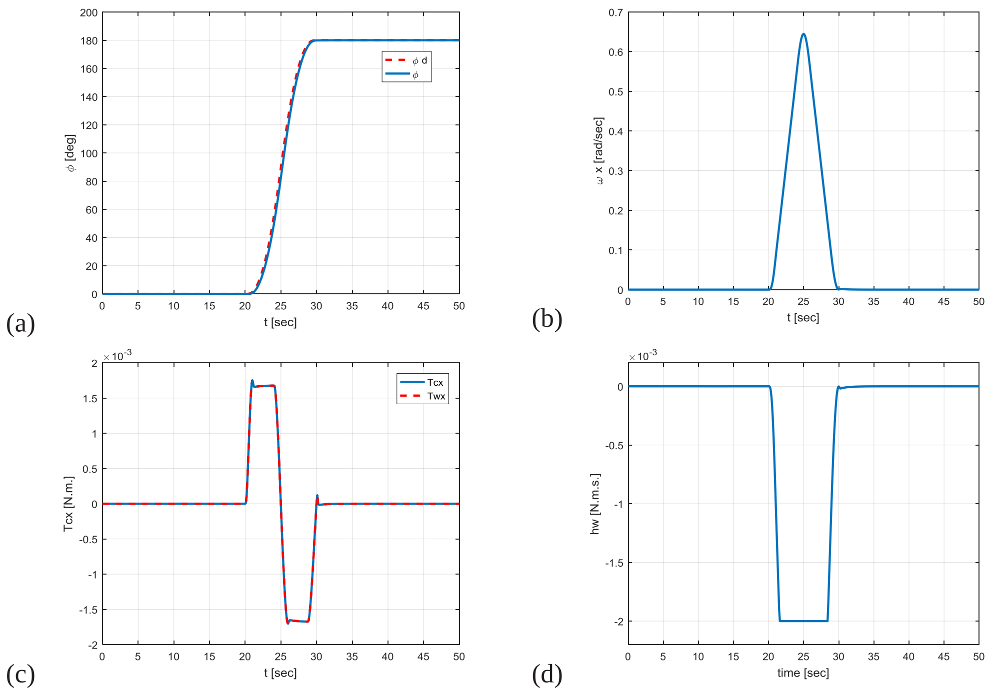

Figure 7-34**:** (a) desired angle and rotation angle about X-axis (φ), (b) angular velocity, (c) input control torque and reaction wheel torque, (d) reaction wheel momentum

7.5.5. Simulation results by one reaction wheel and three magnetorquers

In this section, the performance of proposed controller is presented to the satellite attitude control by three magnetorquers mounted on each main axis and one reaction wheel mounted on Y-axis. In this case, the wheel distribution matrix is defined as

$$D = \begin{bmatrix} 0 & 0 & 0 \\ 0 & 1 & 0 \\ 0 & 0 & 0 \end{bmatrix} \tag{7-8}$$

As it mentioned, three magnetorquers laid on each axis are used. So, M vector can be obtained as

$$\mathrm{M} = \frac{\mathrm{B(b)}^{\mathrm{T}}}{|\mathrm{b}|^2}\mathrm{Tc} \tag{7-9}$$

Where T_c is desired control torque produced by controller, b is the Earth's magnetic field intensity with respect to the body coordinates and B(b) matrix is explained by Eq. (5-2). The inverse of B(b) isn't used because this matrix is singular.

Desired control torque is obtained from the sum of torques generated by magnetorquers and reaction wheel ($T_c = T_m + T_w$), where T_m is the torque generated by magnetorquer and T_w is the torque generated by reaction wheel. T_m can be obtained as

$$T_m = B(b)\, M \tag{7-10}$$

And T_w can be obtained as

$$T_w = T_{c_y} - T_{m_y} \tag{7-11}$$

Where T_{my} is the torque generated by magnetorquer on Y-axis and T_{cy} is desired control torque on Y-axis produced by controller.

The proposed controller performance is investigated for [0, 90, 0] rotations around z, y, x axis, respectively. As shown in Figure 7-35, the system rotates 90 degrees around y-axis and it could track the desired angle, the angular velocity converges to zero and the torque generated in the satellite is in the limitation range.

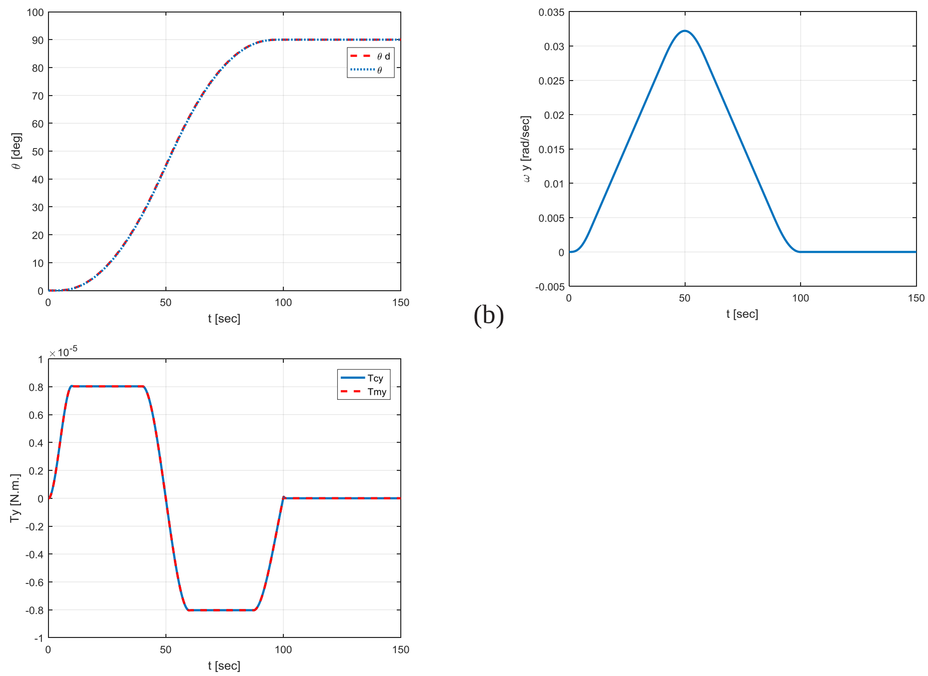

(a) (b) (c)

Figure 7-35: (a) desired angle and rotation angle about Y-axis (θ), (b) angular velocity, (c) input control torque and torque generated in the satellite

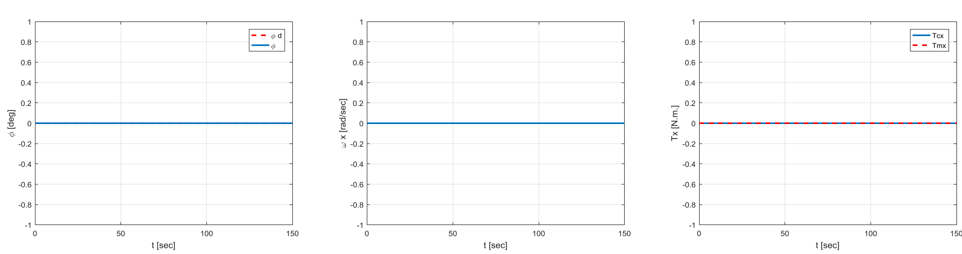

(a) (b) (c)

Figure 7-36: (a) desired angle and rotation angle about X-axis (φ), (b) angular velocity, (c) input control torque and torque generated in the satellite

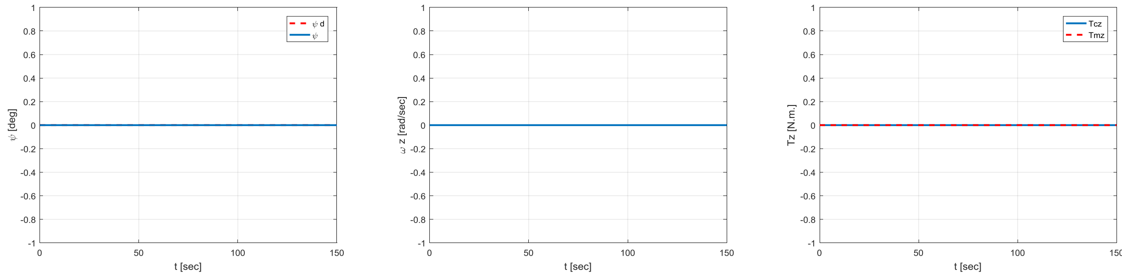

(a) (b) (c)

Figure 7-37: (a) desired angle and rotation angle about Z-axis (ψ), (b) angular velocity, (c) input control torque and torque generated in the satellite

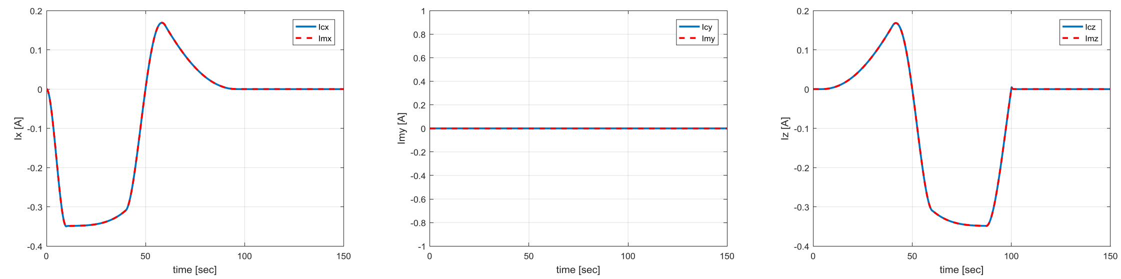

(a) (b) (c)

Figure 7-38: the magnetorquer currents laid on the (a) X-axis, (b) Y-axis, (c) Z-axis

As shown in 7Figure 7-36 and Figure 7-37 angular velocity and rotation angle around X-axis and Z-axis are zero and the controller doesn't generate any torque in X-axis and Z-axis. Magnetorquer current laid on the Y-axis is zero because there is no magnetorquer on this axis.

As shown in Figure 7-38, the magnetorquer current laid on the Y-axis is zero and the magnetorquer currents laid on the X-axis and Z-axis are in the limitation range and converge to zero.

In the next simulation, the desired rotations are chosen [45, 60, 40] degrees about X, Y and Z axes, respectively. Simulation results are shown in Figure 7-39 to Figure 7-42.

It can be seen from Figure 7-39–Figure 7-41(a) that the Euler angles converge to the final desired angles. As shown in Figure 7-39–Figure 7-41 (b), the angular velocities can converge to zero. It can be seen from Figure 7-39–Figure 7-41(c) that actuator input constraints are considered; but, the torques generated by the actuators are not equal to the desired control torque.

As shown in Figure 7-42, the current of magnetorquers are in the limitation range and converge to zero.

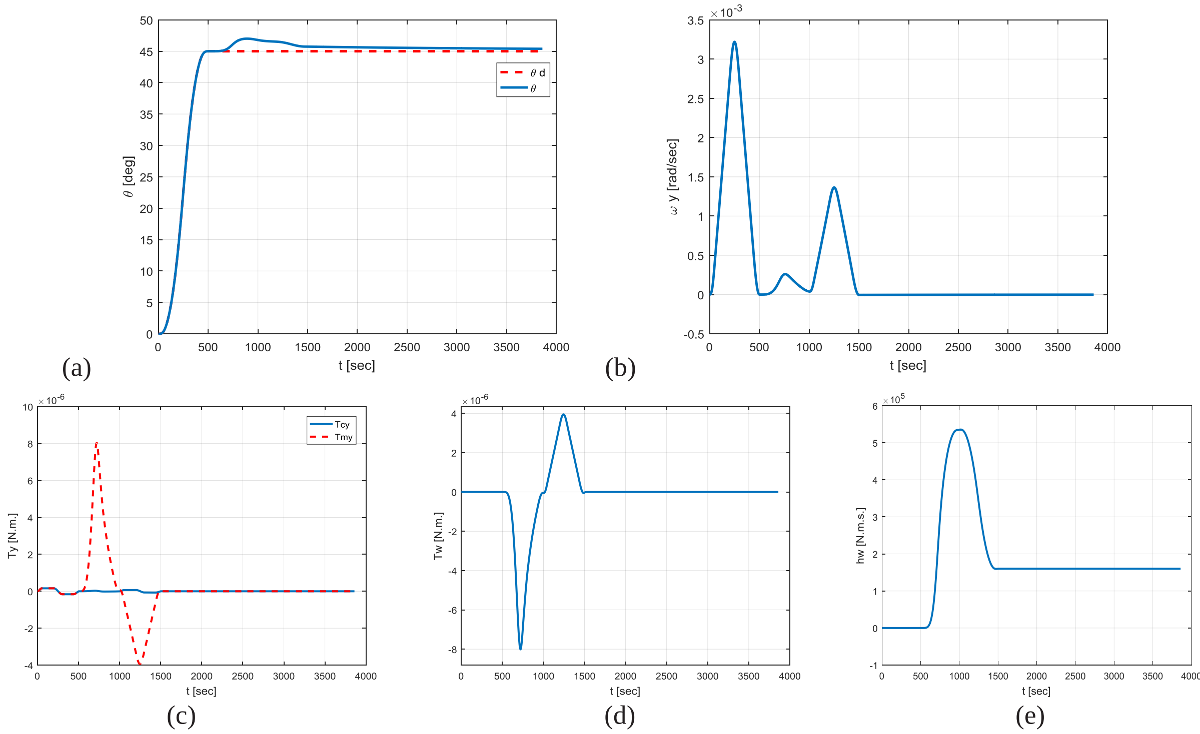

Figure 7-39: (a) desired angle and rotation angle about Y-axis (θ), (b) angular velocity, (c) input control torque and magnetorquer torque, (d) reaction wheel torque, (e) reaction wheel momentum

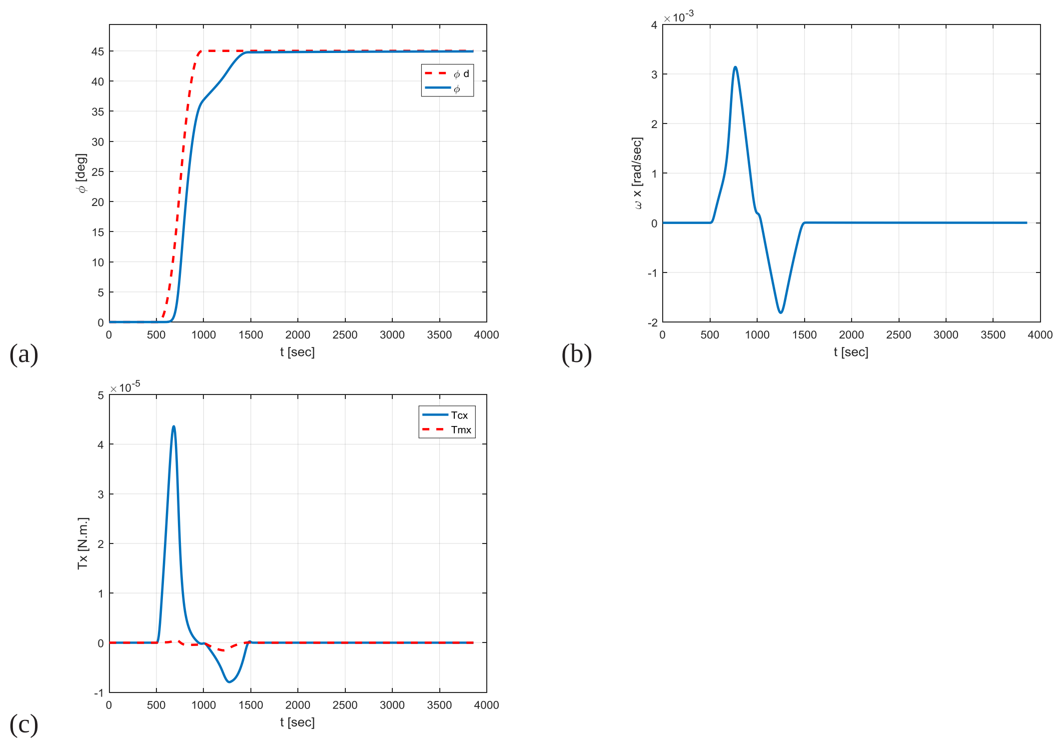

Figure 7-40: (a) desired angle and rotation angle about X-axis (φ), (b) angular velocity, (c) input control torque and magnetorquer torque

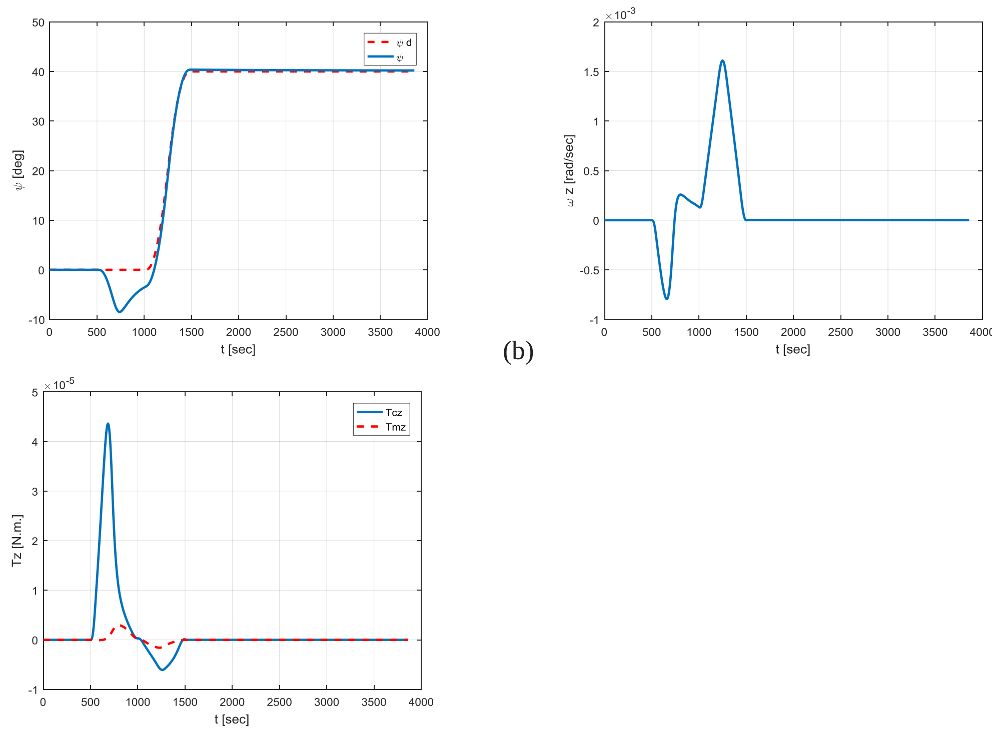

Figure 7-41: (a) desired angle and rotation angle about Z-axis (ψ), (b) angular velocity, (c) input control torque and magnetorquer torque

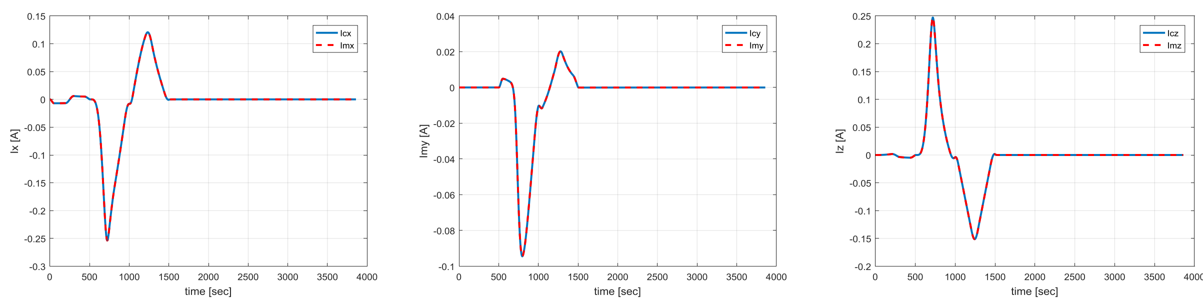

(a) (b) (c)

Figure 7-42: the magnetorquer currents laid on the (a) X-axis, (b) Y-axis, (c) Z-axis

8. Conclusion and future works

In this work, attitude control system for nanosatellites with reaction wheel and magnetorquer actuators is investigated. The control strategy is based on SMC method. Common reference frames, classifications of satellite orbits and orbital elements, magnetic field of earth, types of satellite attitude expression, satellite kinematic and dynamic equations, types of attitude actuators are reviewed before designing controller. The controllers are designed according to the actuator type. Also, actuator input constraints are considered. The simulation results show that the controller could track any desired angle rotation well. The angular velocities can converge to zero.

As part of the future work, the controller can be applied to the satellite located in different orbits with several combinations of the actuators. Also, the robustness of the controller can be tested in presence of the inertia matrix uncertainties and other uncertainties. The controller can be implemented and evaluated on a simulator as a future work. Adaptive Sliding Mode Control can be designed as satellite attitude control, simulated and evaluated its performance in presence of unexpected disturbances, uncertainties. Also, a SMC approach can be designed for flexible satellite as a future work.

References

1. Neil Ashby, *The Sagnac effect in the Global Positioning System*, in *Relativity in Rotating Frames: Relativistic Physics in Rotating Reference Frames*, Guido Rizzi and Matteo Luca Ruggiero, Editors. 2004, Kluwer Academic Publishers, Springer. p. 11.
2. Leonardo M. Reyneri, *Attitude and Orbit Determination and Control of Small Satellites*. 2017.
3. Sybil P. Parker, *McGraw-Hill Dictionary of Scientific and Technical Terms Sixth Edition*. 2002, McGraw-Hill. p. 1772.
4. M. J. SIDI, *Spacecraft Dynamics and Control*. 1997: Cambridge University Press.
5. Shubham Paul. *Calculation of Right Ascension and Declination and its conversion to Azimuth and Altitude [Calculated using Kepler's Laws] using Osculating Elements*. 2016.
6. G S Rao, *Global Navigation Satellite Systems*. 2010: Tata McGraw-Hill Education.
7. R. Nagarajan, *Drought Assessment*. 2010: Springer Science & Business Media.
8. Jaan Praks, Hannu Koskinen, and Zainab Saleem, *Celestial Mechanics and Satellite Orbits*. 2017.
9. J. R. WERTZ, *SPACECRAFT ATTITUDE DETERMINATION AND CONTROL*. 1978: library of Congress Cataloging in Publication Data.
10. W. G. Breckenridge, *Quaternions proposed standard conventions*, in *NASA Jet Propulsion Laboratory,Technical Report*. Oct. 1979.
11. NASA Mission Planning and Analysis Division, *Euler Angles, Quaternions, and Transformation Matrices*. Retrieved 12 January 2013.
12. Blanco, J.-L., *A tutorial on se (3) transformation parameterizations and on-manifold optimization*. 2010.
13. *NSS Magnetorquer Rod*. Available from: https://www.cubesatshop.com/product/nss-magnetorquer-rod/.
14. Max Pastena and James Barrington-Brown, *Comparison of Magnetorquer Performance.* Presentation to CubeSat Workshop, 8th August 2010.
15. Vincent Francois-Lavet, *Study of passive and active attitude control systems for the OUFTI nanosatellites*, in *Faculty of Applied Science*. 2010, university of LIEGE, Belgium.
16. Q. Hu, *Robust adaptive sliding-mode fault-tolerant control with L-gain performance for flexible spacecraft using redundant reaction wheels.* IET Control Theory Appl., 2010. **4**(6): p. 1055-1070.
17. *RSI 45 Momentum and Reaction Wheels*. Available from: https://www.rockwellcollins.com/Products_and_Services/Defense/Platforms/Space/RSI_45_Momentum_and_Reaction_Wheels.aspx.
18. Jean-Jacques E. Slotine and Weiping Li, *Applied Nonlinear Control*. 1991: Prentice Hall.
19. Hassan K. Khalil, *Nonlinear systems*. 2002: Prentice Hall.
20. Vadim Utkin, *SLIDING MODE CONTROL.* CONTROL SYSTEMS, ROBOTICS AND AUTOMATION. **XIII**.
21. Ismail Bendaas and Farid Naceri, *A New Method to Minimize the Chattering Phenomenon in Sliding Mode Control Based on Intelligent Control for Induction Motor Drives.* SERBIAN JOURNAL OF ELECTRICAL ENGINEERING June 2013. **10, No.2**: p. 231-246.
22. H. Lee and Y. Kim, *Fault-Tolerant control scheme for satellite attitude control system.* IET Control Theory and Applications, 2009.